Biomass-burning and urban emission impacts in the Andes Cordillera region based on in-situ measurements from the Chacaltaya observatory, Bolivia (5240 m a.s.l.)

Chauvigné Aurélien[1,11~~10~~], Diego Aliaga[2], Karine Sellegri[1], Nadège Montoux[1], Radovan Krejci[3], Griša Močnik[4], Isabel Moreno[2], Thomas Müller[5], Marco Pandolfi[6], Fernando Velarde[2], Kay Weinhold[5], Patrick Ginot[7], Alfred Wiedensohler[5], Marcos Andrade[2,8], Paolo Laj[7,~~9~~8,~~10~~9]

[1] Laboratoire de Météorologie Physique, OPGC, CNRS UMR6016, Université d'Auvergne, Clermont-Ferrand, France
[2] Laboratorio de Física de la Atmósfera, Universidad Mayor de San Andrés, La Paz, Bolivia
[3] Department of Environmental Science and Analytical Chemistry & Bolin Centre of Climate Research, Stockholm University, Stockholm 10691, Sweden
[4] Condensed Matter Physics Department, Jožef Stefan Institute, Ljubljana, Slovenia
[5] Leibniz Institute for Tropospheric Research, Permoserstr. 15, 04318 Leipzig, Germany
[6] Institute of Environmental Assessment and Water Research, c/ Jordi-Girona 18-26, 08034, Barcelona, Spain
[7] Univ-Grenoble-Alpes, CNRS, IRD, Grenoble-INP, IGE, 38000 Grenoble, France
[8] Department of Atmospheric and Oceanic Science, University of Maryland, College Park, MD, USA
[~~9~~8] CNR-ISAC, National Research Council of Italy – Institute of Atmospheric Sciences and Climate, Bologna, Italy
[~~10~~9] University of Helsinki, Atmospheric Science division, Helsinki, Finland
[11] Now at : Laboratoire d'Optique Atmosphérique, CNRS UMR8518, Université de Lille, Lille, France

Correspondence to: Aurélien Chauvigné (aurelien.chauvigne@univ-lille.fr)

Abstract. This study documents and analyzes a 4-year continuous record~~We present the variability~~ of aerosol optical properties ~~aerosol particle optical properties~~ measured at the Gglobal Atmosphere Watch (GAW) station of Chacaltaya (5240 m a.s.l.), in Bolivia. Records of Particle light scattering and particle light absorption coefficients are used to investigate how the high Andean cordillera is affected by both long-range transport and by the fast-growing agglomeration of La Paz / El Alto, located approximately 20 km away and 1.5 km below the sampling site. The ~~in-situ mountain site is ideally located to study regional impacts of the densely populated urban area of La Paz/El Alto, and the intensive activity in the Amazonian basin. Four year measurements~~extended multi-year allows to study the properties of aerosol particle ~~properties~~ for different air-mass ~~origins~~types, during wet and dry ~~as well as for wet and dry~~ seasons, ~~including~~ also covers periods with the site affected by biomass-burning ~~influenced periods~~in the Bolivian lowlands and the Amazonian basin~~, layers~~. The absorption, scattering and extinction coefficients (median annual values of 0.74, 12.14 and 12.96 Mm^{-1} respectively) show a clear seasonal variation with low values during the wet season (0.57, 7.94 and 8.68 Mm^{-1} respectively) and higher values during the dry season (0.80, 11.23 and 14.51 Mm^{-1} respectively). The record is driven by variability at both seasonal and diurnal scales. At diurnal scale, all records of intensive and extensive aerosol properties show a pronounced variation (daytime maximum, nighttime minimum), as a result of the dynamic and convective effects. The particle light absorption, scattering and extinction coefficients are on average 1.94, 1.49 and 1.55 times higher, respectively, in the turbulent thermally driven conditions as respect to the more stable condition, due to more efficient transport from the boundary layer. Retrieved intensive optical properties are significantly different from one season to the other, reflecting the changing aerosol emission sources of aerosol at larger scale.~~These parameters also show a pronounced diurnal variation (maximum during daytime, minimum during nighttime, as a result of the dynamic and convective effects of leading to lower atmospheric layers reaching the site during daytime. Retrieved intensive optical properties are significantly different from one season to the other, showing the influence of different sources of aerosols according to the season. Both intensive and extensive optical properties of aerosols were found to be different among the different atmospheric layers. The particle light~~

~~absorption, scattering and extinction coefficients are in average 1.94, 1.49 and 1.55 times higher, respectively, in the turbulent layer compared to the stable layer. We observe that the difference is highest during the wet season and lowest during the dry season.~~ Using wavelength dependence of aerosol particle optical properties, we discriminated contributions from natural (mainly mineral dust) and anthropogenic (mainly biomass-burning and urban transport or industries) emissions according to seasons and ~~tropospheric layers~~local circulation. The main sources influencing measurements at CHC are ~~arising~~ from the urban area of La Paz/El Alto in the Altiplano, and regional biomass-burning from the Amazonian basin. Results show a 28% to 80% increase in~~of~~ the extinction coefficients during the biomass-burning season with respect to the dry season, which is observed in both tropospheric dynamic ~~layers~~conditions. From this analysis~~ze~~, long-term observations at CHC provides the first direct evidence of the impact of Biomass Burning emissions of~~in~~ the Amazonian basin and urban emissions from La Paz area on atmospheric optical properties to a remote site ~~far away from their sources,~~ all the way to the ~~stable layer~~free troposphere.

Introduction:

Natural and anthropogenic aerosol particle emissions significantly influence the global and regional climate by absorbing and scattering ~~the~~ solar radiation (Charlson et al., 1992; Boucher et al., 2013; Kuniyal et Guleria 2018). Global-scale estimates of aerosol radiative forcing are still highly uncertain. Regional and local scale radiative forcing estimates show large variability~~ies~~, reflecting the dependence on highly variable factors such as the ground albedo, aerosol particle loadings, as well as the nature and localization of the aerosol particle in the atmosphere. While aerosol particles have a net cooling effect at a global-scale (-0.35 $W.m^{-2}$, Myrhe et al., 2013), the sign of local direct radiative forcing is determined by a balance between cooling by most aerosol species (sulfates, nitrates, organic aerosols and secondary organic aerosols), and warming by black carbon (BC) that absorbs solar radiation (Myhre et al., 2013).

The major sources of BC particles are biomass-burning and incomplete fuel combustion. The Amazonian Basin accounts for approximatively fifty percent of the global tropical forest area and shrink more than 2% every year, which makes it ~~the~~ one of the most important sources of BC particles. However, long term measurements at high altitude are still poorly documented in this region. Some observations of regional aerosol burden show the intense emission sources for both primary and secondary aerosol particle and their local impacts. Martin et al. (2010) report evidence of natural and anthropogenic emissions in this region with clear seasonal variations of atmospheric particle concentrations close to the surface. Artaxo et al. (2013) retrieved from a sampling location close to nearby recurrent fires (close to Porto Velho) concentrations of biomass particles 10 times higher during the dry period than during wet period. The authors also report that the particles concentrations at this site are 5 times higher than at a remote site in the same area, and both sites show a clear seasonal variation.

In addition to the aforementioned studies on the aerosol burdens, several other studies show important modifications of the atmospheric optical properties during biomass-burning (BB) episodes, in the Amazonian basin and in la Plata basin at the end of the dry season (August - September). Between the wet season and the biomass burning season, Schafer et al. (2008) show an increase of Aerosol Optical Depth by a factor of 10 from AERONET sites in southern forest region and the Cerrado region and, by a factor of 4 in the northern forest region. Husar et al. (2000) have reported extinction coefficients on the integrated visible range (or visibility) in the Amazon basin at four different altitude stations during the BB period. The study reports a spatial pattern of the ~~extinction coefficient between~~ visibility between 100 and 200 Mm^{-1} over the Amazon Basin. However, ~~extinction coefficient~~ values can reach 600 Mm^{-1} at Sucre station (2903 m above sea level, hereafter abbreviated as "a.s.l."), 1000 Mm^{-1} at Vallegrande (1998m a.s.l.) and 2000 Mm^{-1} at Camiri (792 m a.s.l.) during BB period. Even the study clearly shows impacts of Amazonian activities at different altitudes and long distances, only few studies report long time period of aerosol optical properties. At "Fazenda Nossa Senhora Aparecida" (FNSA) station in Brazil (770 m a.s.l.), Chand et al. (2006) report the absorption and scattering coefficients reaching 70 Mm^{-1} (at 532 nm) and 1435 Mm^{-1} (at 545 nm) respectively during large-scale BB events (PM2.5 > 225µg.m^{-3}) from ground-based

measurements. ~~This significant difference~~These extremely high coefficients ~~is~~ are due to the proximity to BB sources for FNSA station and its very low altitude.

Only a few studies report BC transport through different atmospheric layers. During the Large-Scale Biosphere-Atmosphere Experiment in Amazonia (LBA, in March 1998), Krejci et al. (2003) retrieved particle concentrations in the free Tropospheric Layer (above 4 km a.s.l.), 2 and 15 times higher than in the boundary layer, due to new particle formation in BB plumes. From airborne LIDAR measurements during SAMBBA, Marenco et al. (2016) have also observed high particle concentrations at high altitude (between 1 to 6 km). Their work highlight long range transport of biomass-burning plumes with lifetimes of several weeks. Chand et al. (2006) also demonstrate increasing particle scattering with altitude, partly explained by particle coagulation and condensation of gases during transport. Bourgeois et al. (2015) show from satellite remote sensing measurements (Cloud-Aerosol Lidar with Orthogonal Polarization, CALIOP), that BB particles originating from the Amazonian Basin reach the altitude of 5 km a.s.l. Contrary to Krejci et al. (2003) and Chand et al. (2006), they show a constant decrease of aerosol particle extinction with altitude, at a rate of 20 Mm^{-1} per kilometer of altitude. Hamburger et al. (2013) present long term (3 years) ground-based measurements at Pico Espejo (4765 m a.s.l.), Venezuela. They show the influences of the local Venezuelan savannah and of the Amazonian basin biomass Burning emissions, mainly during the dry period, and into the whole Tropospheric layer.

A challenging part is to separate the contributions of different aerosol sources from retrieved optical properties. For example, the single scattering albedo (SSA) is closely related to the particle size, and determines the magnitude of the aerosol radiative forcing (Hansen et al., 1997). For Tropical BB events, the SSA is around 0.83 at 550 nm for a fresh plume and increases with time up to 0.87 (Reid et al., 2005). On the other hand, the spectral dependency~~es~~ of aerosol optical properties, the Angström exponents, decrease during the aging process of the smoke. From five different campaigns over different continents using AERONET sites, Russel et al. (2010) work permits to define thresholds on the absorption and scattering Angström exponents (respectively AAE and SAE) for urban pollution, BB and dust particles. They associated urban pollution particles to AAE close to 1, whereas BB particles to AAE close to 2. In addition, SAE values are close to 1 for Dust particles and close to 2 for urban particles. Similar results are observed from Clarke et al. (2007) work, based on in-situ airborne measurements over North-America. Their work show BB plumes with AAE values close to 2,1 and polluted plume with AAE close to 1. The correlation between the single scattering albedo Angström exponent (SSAAE) and the concentration of dust allows to define that air masses with SSAAE values bel~~l~~ow 0 are mainly influenced by dust sources, contrarily to urban pollution sources that show values above 0 (Collaud Coen et al., 2004). This has also been confirmed from different AERONET sites in the world (Dubovik et al., 2002).

Aerosol type	SAE	AAE	SSAAE
Dust	Close to 1	Close to 1	Below 0
Urban pollution	Close to 2	Close to 1	Higher than 0
Biomass burning		Close to 2,1	

Table 1: Expected aerosol type and their optical properties for each cluster according season and atmospheric stability.

As a summary, Table 1 shows expected Angström exponent for dust, urban pollution and Biomass Burning particles according the different referenced works (Dubovik et al., 2002 ; Collaud Coen et al., 2004 ; Clarke et al., 2007 ; Russel et al., 2010). This information has to be taken with caution since source influences are expected homogeneous and have been reported from several regions.

The present work aims at evaluating the contribution of anthropogenic and natural particle to the global optical properties of aerosols measured at a high altitude background site at Chacaltaya (Bolivia) over a four-year period (2012-2015). Monthly and diurnal variations of extensive optical properties (related to particle concentration) and intensive optical properties (related to particle chemistry) are firstly shown.~~allow as a first step to analyze seasonal~~

~~variation of both anthropogenic and natural emissions in this region. Because aerosol particle transported within the atmospheric layers is still weakly studied,~~A ~~a~~ robust method based on the measurement of the atmospheric stability is then applied to distinguish atmospheric ~~layer~~conditions (stable and turbulent). ~~In addition~~Finally, ~~a~~ back-trajectory analysis and optical wavelength dependences are presented to identify~~ies~~ impacts of local and regional aerosol sources ~~that gives impacts to the area in these different atmospheric layers~~.

1. Site description

The urban area of La Paz/El Alto, extends from approximately 3200 m to more than 4000 m a.s.l. in the Altiplano. It is a fast growing urban area with a population of c.a. 1.7 million inhabitants, covering a complex topography. In this region, meteorological conditions are governed by wet and dry seasons. The wet season span~~is~~ from December to March, and the dry season from May to September. April, October and November are considered as transition periods between the two main seasons. ~~During August and September~~Between May and October, agricultural practices in the Yungas ~~and Zongo Valleys~~ (closest valleys to the La Paz plateau and the Amazonian Basin) and the Amazon and La Plata basins include intense vegetation burning~~.~~ (Carmona-Moreno et al. 2005, Giglio et. al 2013). Indeed, the closest region where large areas are affected by biomass burning activities is the Bolivian Amazonia (Beni, Santa Cruz, north of La Paz departments) located ca. 300 km from the station, north and eastward from the Andes mountain range. In this paper, were choose to ~~therefor~~ define August and September as the biomass-burning (BB) period because those are the months when the BB activities are more intense in the aforementioned region.~~.~~

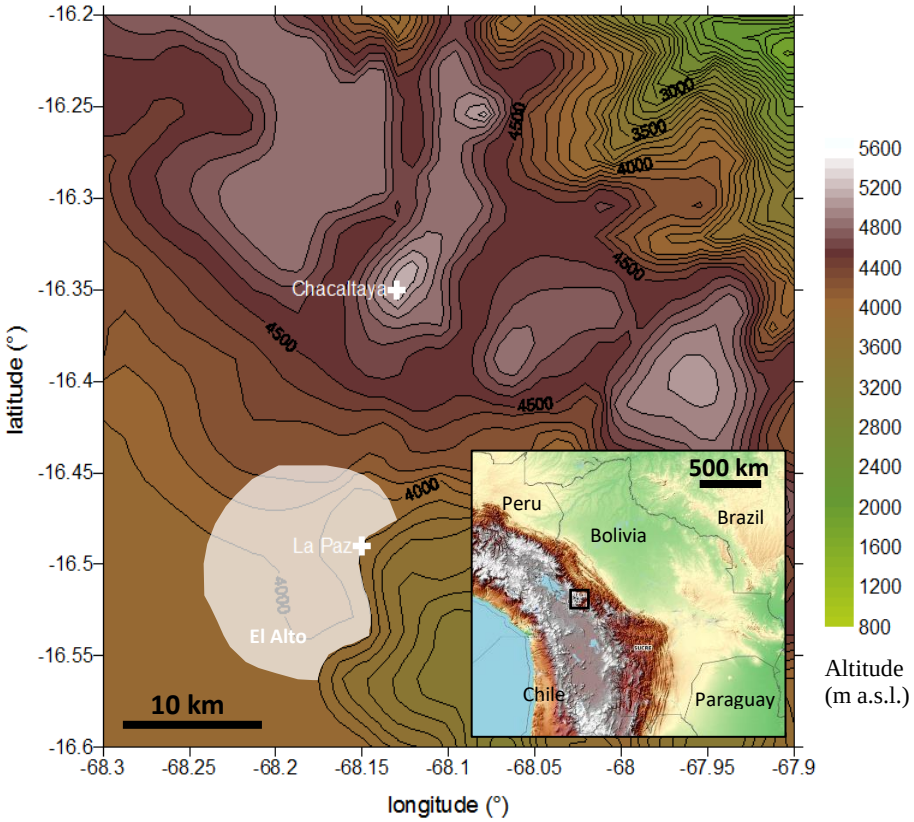

Figure 1: Topographic ~~situation~~ description of La Paz and Chacaltaya region, and Bolivia in the lower right panel. The black rectangle on the small panel represents ~~the~~ La Paz region. The urban area of La Paz-El Alto (marked as white shading) lies in the Altiplano high-plateau at around 4000 m a.s.l..

The in-situ measurement site used in this study is the high altitude station of Chacaltaya GAW (Global Atmospheric Watch) (site code: CHC, and coordinates: 16°21 S, 68°07 W), located at 5.240 m a.s.l., at 17 km North of La Paz, as shown in Fig. (1). In-situ instruments of the station operated behind a Whole Air Inlet equipped with an automatic dryer (activated above 90% RH). T~~T~~he station continuously measures concentrations of trace

gases, and physical and chemical properties of aerosols since 2011 (Rose et al., 2015). In the current study, the full dataset of in-situ optical measurements has been used between January 2012 and December 2015.

2. Instrument and methods

2.1. In-situ measurements

Absorption and scattering coefficients of the aerosol were measured in dry conditions (< 40 %) using an Aethalometer (Magee Scientific AE31) at 7 different wavelengths (370, 470, 520, 590, 660, 880 and 950 nm), a Multi-Angle Absorption Photometer (MAAP, Thermo Scientific) at 635 nm and an integrated Nephelometer (Ecotech Aurora 3000) at 3 wavelengths (450, 525 and 635 nm). The Aethalometer measures the rate of change of optical transmission of the filter on which particles are collected at 5-minute resolution. Every 5 minutes, the spot on the filter band is changed in order to reduce loading effects. The reference of the transmissivity is the part of the same filter without particles (Hansen et al., 1982). Sensor calibration is performed automatically and an uncertainty of 5 % on attenuation coefficients is given by the constructor. Aethalometer measurements were compensated for multi-scattering effects and loading effects (or shadowing effects) ~~with~~ following the method described by Weingartner et al. (2003) briefly explained below. As described by Weingartner et al. (2003) and ~~re~~used on Chacaltaya measurements by Rose et al. (2015), the absorption coefficient σ_{abs} is retrieved from BC concentrations measured from the aethalometer. From BC concentrations at every measurement spots, attenuation coefficients σ_{atn} at different wavelengths are retrieved as:

$$\sigma_{atn}(\lambda) = BC(\lambda) \,.\, \sigma_{m}(\lambda) \quad (1)$$

with σ_m the mass coefficients given by the instrument's instructions (The Aethalometer, A.D.A. Hansen, Magee Scientific Company, Berkley, California, USA) and based on the Mie theory. σ_m strongly depends on the aerosol type and age (from 5 to 20 $m^2\ g^{-1}$, Liousse et al., 1993). However, the manufacturer values (14625 nm $m^2\ g^{-1}\ \lambda^{-1}$) have been recently validated in a comparison study between different aethalometer corrections (Collaud Coen et al., 2010 ; Saturno et al., 2017).~~.~~

The absorption coefficient is then calculated with the following equation:

$$\sigma_{abs}(\lambda) = \frac{\sigma_{atn}(\lambda)}{C.R(\lambda)} \quad (2)$$

with C = 3.5 a calibration factor linked to multiple-scattering and assumed constant according wavelengths (GAW Report No. 227),

and R, a calibration factor which depends on aerosol loading on the filter and aerosol optical properties, ~~-~~calculated as:

$$R(\lambda) = \left(\frac{1}{f(\lambda)} - 1\right) \frac{\ln(\sigma_{atn}(\lambda)) - \ln(10\%)}{\ln(50\%) - \ln(10\%)} + 1 \quad (3)$$

where f is the filter loading effect compensation parameter and represents the slope of the curve of R as~~in~~ function of $\ln(\sigma_{atn})$ for a σ_{atn} change from 10% to 50% . This factor is adjusted to obtain a median ratio between the absorption coefficient before and after spot changes close to 1.

Similarly to the Aethalometer, the MAAP measures the radiation transmitted and scattered back from a particle-loaded fiber filter (Petzold and Schönlinner, 2004). According to Petzold and Schönlinner (2004), uncertainty of the absorbance is 12%. A mass absorption cross-section Q_{EBC} = 6.6 $m^2.g^{-1}$ at 670 nm is used to determine Equivalent Black Carbon mass concentrations (m_{EBC}) from absorption coefficient (σ_{abs}) and a wavelength correction factor of 1.05 was applied according Equ. (4) to obtain σ_{abs} at 635 nm (Müller et al., 2011a) from measurement at 637 nm.

$$\sigma_{abs} = 1.05\, m_{EBC}\, Q_{EBC} \quad (4)$$

The nephelometer measures the integrated light scattered by particles. Because the angular integration is only partial (from 10° to 171°), nephelometer data were corrected for truncation errors, but also for detection limits

according to Müller et al. (2011b). The instrument permits to retrieve aerosol particle scattering coefficients (σ_{scat} from 10° to 171°). The nephelometer instrument is calibrated using CO2 as span gas and frequent zero adjusts were performed, following the procedure described in Ecotech manual (2009). The uncertainty of the Aurora 3000 is given in the user manual to be 2,5 %. However, it has been noticed that the three wavelengths of the Chacaltaya's nephelometer do not present equivalent robustness. Indeed, measurements at 635 nm remain unstable during the analyzed period and are thus not selected for the following results.

More optical parameters can be retrieved from the combination of these instruments. The extinction coefficient (σ_{ext}) and aerosol particle single scattering albedo (SSA) are calculated according to Equ. (5) and (6). In addition, the full spectral information of each instrument is fitted by a power-law (Equ. (7) and (8)) and allow to retrieve aerosol particle Angström exponents such as the scattering Angström exponent (SAE) from nephelometer measurements, the absorption Angström exponent (AAE) from aethalometer measurements and the single scattering albedo Angström exponent (SSAAE).

$$\sigma_{ext}(\lambda) = \sigma_{abs}(\lambda) + \sigma_{scat}(\lambda) \quad (5)$$

$$SSA(\lambda) = \frac{\sigma_{scat}(\lambda)}{\sigma_{scat}(\lambda) + \sigma_{abs}(\lambda)} \quad (6)$$

$$\sigma_{abs}(\lambda) = b_{abs} \times \lambda^{-AAE} \quad (7)$$

$$\sigma_{scat}(\lambda) = b_{scat} \times \lambda^{-SAE} \quad (8)$$

$$SSA(\lambda) = b_{ssa} \times \lambda^{-SSAAE} \quad (9)$$

With b_{abs}, b_{scat} and b_{ssa},and AAE, SAE and SSAAE the power-law fit coefficients.

2.2. Method for differentiating stable or turbulent conditions at CHC

As is often the case for ~~a~~ mountain sites, CHC is strongly influenced by thermal circulation, developed~~ing~~ on a daily basis on mountain slopes (Whiteman, 2000). Depending on the time of the day and the season, the CHC high-altitude site ~~at CHC~~ can be influenced ~~measure the~~by air-masses from the mixing layer, the r~~R~~esidual l~~L~~ayer ~~(RL)~~ or the lower f~~F~~ree t~~T~~roposphere. The mixing layer height is driven by convective processes related to surface temperature, with higher mixing layer height during daytime and lower height during nighttime. In addition to the diurnal mixing layer cycle, the complex mountainous topography of the area affects ~~regional~~ local circulation by channeling the air flow, thus complicating the differentiation between the mixing layer and free troposphere. In addition, a residual layer can also be present at CHC station during nighttime, resulting from low dispersion of the daytime convection. Because no clear distinctions between the mixing, the free tropospheric, and the residual layers can be strictly obtained from in-situ measurements only, the present dataset recorded at Chacaltaya station is separated in terms of stability conditions (turbulent and stable). To differentiate stable conditions (~~SL~~SC; typically the free Tropospheric layer, but also RL) from turbulent conditions (~~TL~~TC; typically the mixing layer, but also cloudiness over the station or wind channelling effects), we used a methodology described in Rose et al. (2017). This method is based on the hourly averaged value of the standard deviation of the horizontal wind direction (σ_θ in Eq. 10) calculated every 15 minutes:

$$\sigma^2_{\theta(1h)} = \frac{\sigma^2_{\theta(15)} + \sigma^2_{\theta(30)} + \sigma^2_{\theta(45)} + \sigma^2_{\theta(60)}}{4} \quad (10)$$

with $\sigma_{\theta(15)}$ the standard deviation of the horizontal wind direction calculated on the first 15 minutes of every hour, and $\sigma_{\theta(60)}$ the last 15 minutes of every hour.

$$\sigma_\theta = \sin^{-1}(\varepsilon)[1.0 + b\varepsilon^3] \quad (11)$$

and b = $2/\sqrt{3} - 1 = 0.1547$, $\varepsilon = \sqrt{1-(s_a^2 + c_a^2)}$ ~~$= 1 - (s_a^2 + c_a^2)$~~

~~,~~with the averages $s_a = \frac{1}{N}\sum_{i=1}^{N} sin\theta_i$ ~~s_a~~ and $s_a = \frac{1}{N}\sum_{i=1}^{N} cos\theta_i$ ~~c_a~~ of N the number of horitontal wind direction (θ_i) recorded in 15 minutes. ~~the sine and cosine of the 15-minute average wind direction measurements.~~

A smoothed threshold is used to separate ~~TL~~TC and ~~SL~~SC ranges from 12.5° to 18º for the dry season and from 12.5º to 22.5º for the wet season based on Mitchell (1982)'s recommendations and on BC analyses (Rose et al., 2017). Interface cases correspond to unclassified data which mainly show high variability of the standard deviation between the two categories of dynamic. As described in Rose et al. (2017), the classification depends also on the σ_θ value in the 4-hour time interval across the time of interest. Interface cases correspond to unclassified data which mainly show a high variability of the standard deviation between the two categories of dynamic. For clarity, the interface cases are excluded from the dataset in the rest of the paper.

The standard deviation of horizontal wind direction at CHC highlights the diurnal cycle between stable and turbulent conditions directly related to temperature and the behavior of the atmospheric boundary layer (ABL). This influence of the ~~TL~~TC at CHC is due to its particular topographical setting, particularly due to its proximity to the Altiplano plateau (altitude > 3 km, 200 km width near CHC). This high and semiarid plateau receives significant amounts of solar radiation that heat the surface, producing an expansion of the ~~TL~~TC as observed in Lidar measurements near the station (Wiedensohler et al. 2018).

~~For clarity, the residual layer is excluded from the dataset in the rest of the paper.~~

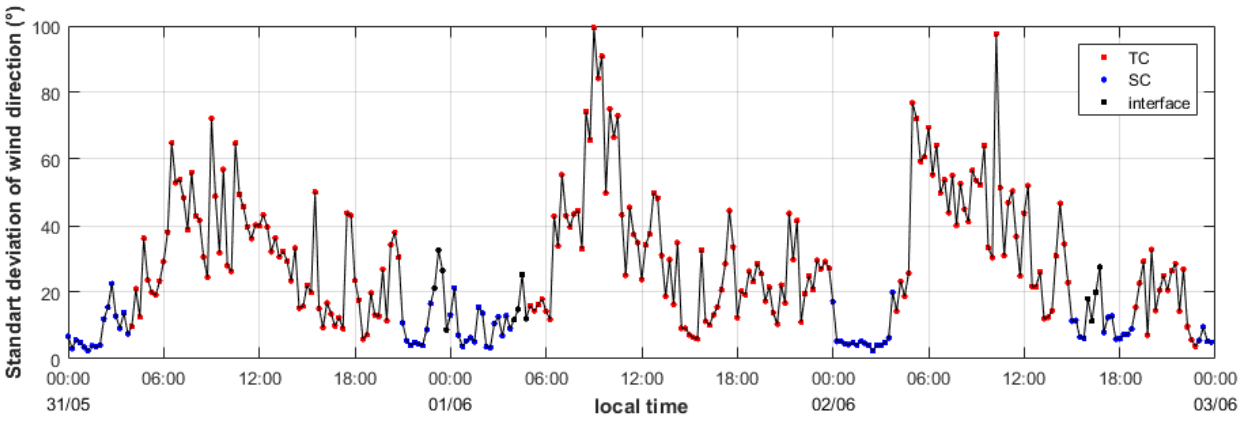

Figure 2: Standard deviation of the wind direction measured at the high altitude site of Chacaltaya (5240 m a.s.l.) from the 31st of May to the 2nd of June 2012 at 1-hour resolution. Red points corresponding to turbulent ~~layer~~ condition (TC~~L~~) cases, blue points to stable ~~layer~~ condition (SC~~L~~) cases and black points to undefined/interface cases. Time corresponds to the local time.

Figure (2) shows the standard deviation of the horizontal wind direction during a 3-day period (from 31 May 2015 to 2 June 2012) with blue lines representing ~~SL~~SC cases and red lines, ~~TL~~TC cases. Black spots represent undefined cases (or interface) due to a fluctuating classification within the 1-hour time window. This 3-day example she~~ows~~ that ~~SL~~SC ~~conditions~~ are mostly observed ~~in the morning~~ during night when the convective effect of the previous day is already dissipated and no convective effect of the current day is present.

Following this classification, the average monthly and diurnal variation of the fraction of ~~SL~~SC, ~~TL~~TC and undefined conditions for each season for 4 years of measurements (from 2012 to 2015) were calculated and are represented in Fig. (3). For each season, ~~SL~~SC ~~conditions~~ are dominant before 10:00 (local time) and after 18:00 whereas ~~TL~~TC ~~conditions~~ are mostly observed during daytime. This tendency is mostly observed during the dry season with more than 60% of ~~TL~~TC ~~conditions~~ in daytime and 80% of ~~SL~~SC ~~conditions~~ in nighttime. However, monthly variations show similar tendencies during the full year with around 60% of time in the stable ~~layer~~condition (~~SL~~SC ~~conditions~~ in blue).

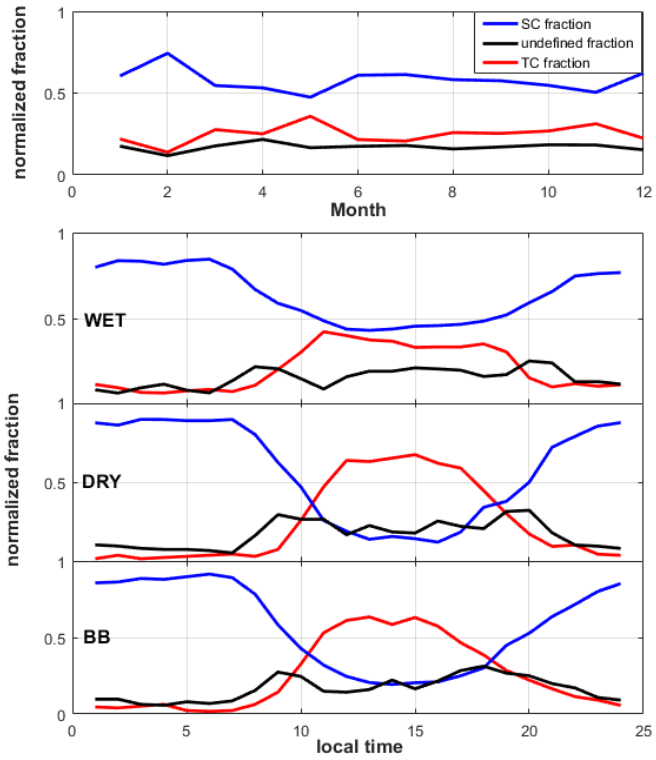

Figure 3: Monthly and diurnal variations of turbulent ~~layer~~ conditions (TC~~L~~, red), stable ~~layer~~ conditions (SC~~L~~, blue) and undefined (black) fractions for each season.

2.3. Identification of air mass origins at regional and meso-scales

HYSPLIT (Hybrid Single Lagrangian Integrate Trajectory, Stein et al., 2015) back-trajectories (BTs) are used in this study to investigate the aerosol particle transport to the CHC station and their properties as a function of the air mass origins. Hence, ~~12 hours and~~ 96 hours air mass BTs are calculated every hour from the CHC station during the four years measurement period (from 2012 to 2015). WRFd04 dataset has been used to generate BTs every hour, starting at nine locations around the Chacaltaya station (within a square of 2x2 km around the station). This dataset presents the best topographic resolution for this region with spatial resolution of 1.06x1.06 km, and 28 pressure levels.

The BTs have been grouped into different clusters defined by their similarities in time and space. The Cluster Analysis method used in this study is described in Borge et al. (2007) and based on the Euclidean geographical coordinates distance and given time intervals. Figure (4a) shows the trajectory frequency plot. The opacity of each pixel is proportional to the number of BTs passing through each grid cell~~pixel. Slow and fast air masses (defined by the mean wind speed through the back-trajectory) are analyzed separately to elaborate on short and long-range influences.~~ . Clusters are defined by using a two-stage technique (based on the non-hierarchical K-means algorithm). Six clusters have been found around the Chacaltaya station. Hence, a fraction of each cluster is assigned to each BT, and is calculated according the residence time in each cluster and their distance from the reference location (the Chacaltaya station)~~Using the method proposed by Borge et al. (2007), a fraction of each cluster is assigned to each BT~~. In order to obtain aerosol optical properties of each cluster, only a part of the back-trajectories have been selected. One BT is selected if its contribution to one cluster is high enough. ~~Thus, f~~For each cluster, the first 10% of the ~~events~~ BTs have been selected by demonstrating the highest contribution to any one cluster~~when the cluster had the most influence in the air masses arriving at CHC~~. This firsts 10% of BTs related to each clusters and their mean paths are shown in Appendix A1.

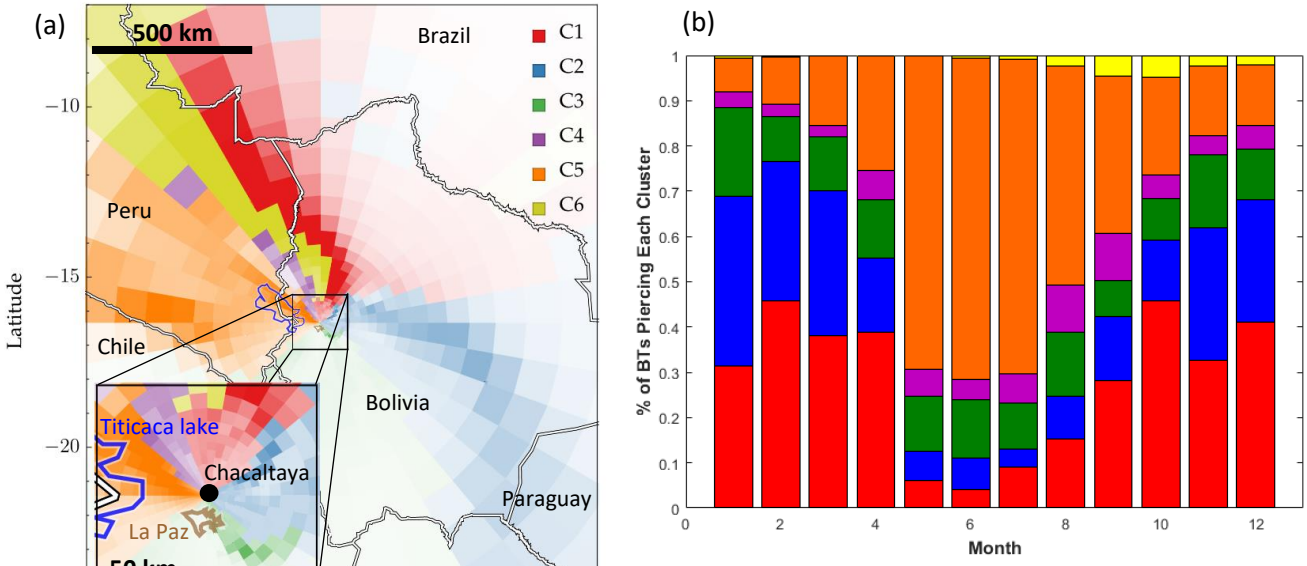

Figure 4: a. Trajectory frequency plot in La Paz region in Bolivia, with a scale of 500 km and 50 km in the lower left corner centered on CHC station. b~~a~~. Monthly variation of the percentage of back-trajectories (BTs) for each cluster. ~~b. Definition of back-trajectory clusters in La Paz region in Bolivia, centered on Chacaltaya station.~~

~~-~~Figure (4b~~a~~) shows seasonal variations of each cluster fraction.

~~Six clusters have been found around the Chacaltaya station and are shown Fig. (4b). The opacity of each pixel is proportional to the number of BTs passing through each pixel.~~ Results show that most of the air-masses influencing the CHC station come from the highlands (Altiplano), the Pacific Ocean, and along the Cordillera Real slopes in the North of the CHC station. For each cluster, a characteristic geolocation along the path of back-trajectory is identified, and acronyms are used for clarity:

- Cluster 1 (NA): Northern Amazonian Basin / North-East slope of Cordillera Real
- Cluster 2 (SA): Southern Amazonian Basin
- Cluster 3 (LP): La Paz / El Alto
- Cluster 4 (ATL): Altiplano / Titicaca lake
- Cluster 5 (APO): Altiplano / Pacific Ocean

- Cluster 6 (NES): North-East slope of Cordillera Real

Clusters 1 and 2 (NA and SA respectively) cover the entire East part of air masses, limited by the high wall formed by the Cordillera Real. These two clusters could be influenced by Amazonian Basin activities, such as BB that is extremely active from August to September, and biogenic forest emissions. Cluster 3 (LP) seems to be the main cluster representing local urban emissions, for example ~~transportation~~vehicle emissions, industrial activities, and domestic heating. Clusters 4 and 5 (ATL and APO) can both give information of Altiplano sources (dust, ~~transport, industrial activities~~urban emissions, …) but also humid air masses from Pacific Ocean and the Titicaca lake. Finally, cluster 6 (NES) has properties close to cluster 1 but with less influence from the Amazonian Basin and close to cluster 4 but with aerosol sources further from CHC station (> 100 km). All these cluster definitions will be discussed in this paper in the context of the associated aerosol particle optical properties.

Figure (4b~~a~~) shows the seasonal influence of the different clusters to CHC measurements. During the dry period, air masses measured at the CHC station are mainly influenced by North-West ~~BTs~~ (cluster APO), according for more than 60% of the BTs between June and July. During the wet period, the main influence is from the East (clusters NA and SA) with more than 60% of the BTs between December and April. Finally, LP, ATL and NES shares about 10% of the BTs throughout the year but with local maximum in August, September and October respectively.

3. Aerosol particle optical properties

3.2. Seasonal and diurnal variations

Monthly median scattering coefficient (σ_{scat}), absorption coefficient (σ_{abs}), extinction coefficient and single scattering albedo (SSA) from 2012 to 2015 are shown in Fig. (5a) with 25^{th} and 75^{th} percentiles. They are all interpolated at 500 nm using scattering and absorption Angström coefficients (Equ. (7) and (8)). Extinction coefficient and SSA were calculated from Equ. (5) and (6) respectively at 500 nm. Figure (5b) shows monthly Angström exponent values from the same dataset.

The annual median [25th percentile – 75th percentile] absorption coefficient at CHC is 0.74 Mm^{-1} [0.43 – 1.25] at 500 nm. A clear seasonal variation can be observed with low values during the wet season (0.57 Mm^{-1} [0.32 – 1.05] between December to March) and higher values during the dry season (0.80 Mm^{-1} [0.52– 1.24] between May and July). The highest values are observed from July to November (including the August-September BB period) with a median absorption coefficient of 1.00 Mm^{-1} [0.64 – 1.70]. Similar seasonal variations are observed for the scattering coefficient, with a more pronounced increase occurring during the BB period.

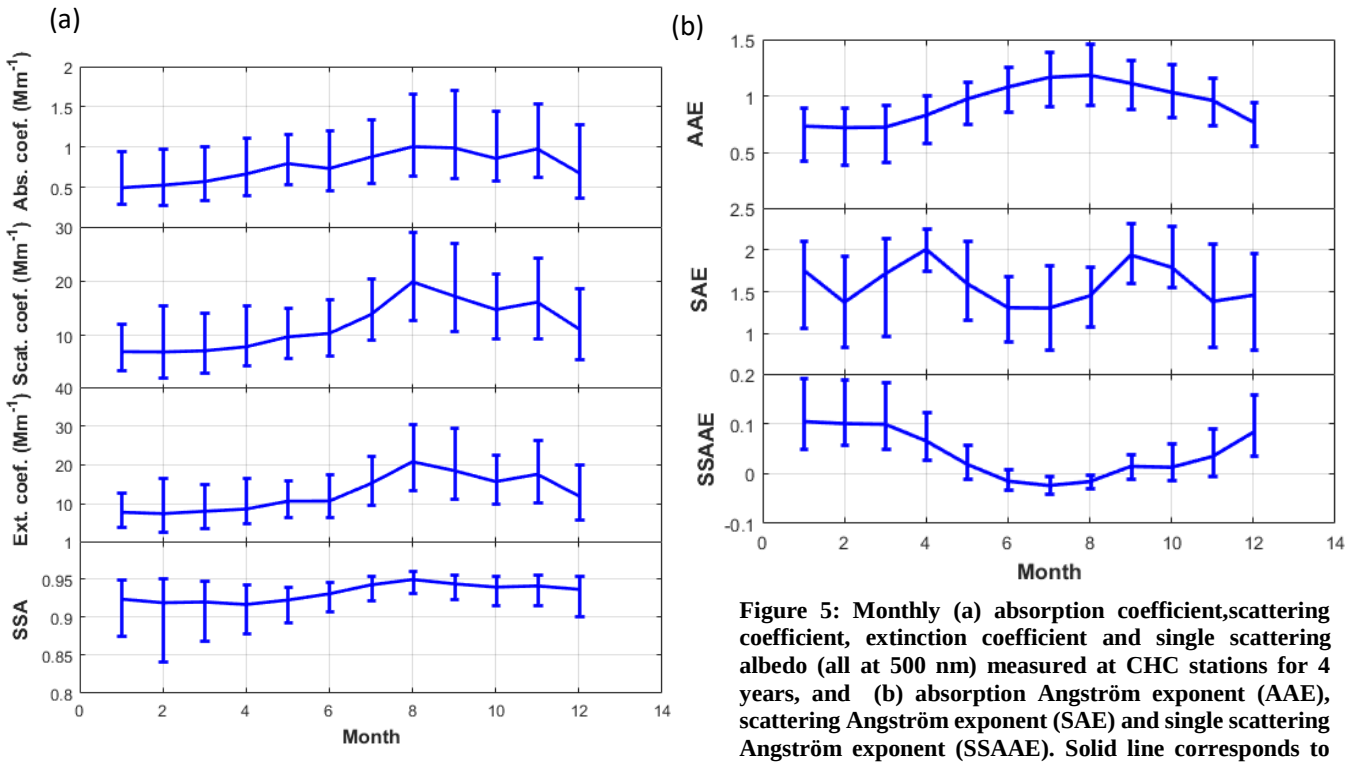

Figure 5: Monthly (a) absorption coefficient,scattering coefficient, extinction coefficient and single scattering albedo (all at 500 nm) measured at CHC stations for 4 years, and (b) absorption Angström exponent (AAE), scattering Angström exponent (SAE) and single scattering Angström exponent (SSAAE). Solid line corresponds to the median and error bars indicate the range between the 25th and 75th percentiles.

The median scattering coefficient of the entire dataset is 12.14 Mm^{-1} [6.55 – 20.17]. Scattering coefficients are lower during the wet season (7.94 Mm^{-1} [3.45 – 15.00]) than during the dry season (11.23 Mm^{-1} [6.94 – 17.60]), and reach a maximum median scattering coefficient of 18.57 Mm^{-1} [11.63 – 28.45] during the BB period. Regardless of the season, these values are very low in comparison to aerosol particle optical properties at lower lying stations, as shown by Chand et al. (2006) during the Large Scale Biosphere-Atmosphere Experiment in Amazonia – Smoke, Aerosols, Clouds, Rainfall and Climate (LBA-SMOCC) campaign at the Fazenda Nossa Senhora Aparecida (FNA) station (10.76°S, 62.32°W, 315 m.s.l.). Their works show that scattering coefficients and absorption coefficients reach 1435 Mm^{-1} and 70 Mm^{-1} respectively during important BB periods while remain at 5 Mm^{-1} and 1 Mm^{-1} during clean conditions.

The median extinction coefficient at CHC is 12.96 Mm^{-1} [7.07 – 21.62] ~~and follows a seasonal variation that is very similar to the one of the scattering coefficient~~. This extinction coefficient range are at least one order of magnitude lower than other measurements reported during the BB period in the Amazonian Basin ~~(up to 2000 Mm^{-1} at Camiri station at 792 m a.s.l., Husar et al., 2000)~~. This is likely due to the altitude at which the CHC station is located and, but mainly, its distance from the BB sources.

We measured a small seasonal variation of the SSA, with a median value of 0.93 [0.87 – 0.95] during wet season, 0.93 [0.91 – 0.95] during dry season and 0.95 [0.93 – 0.96] during the BB period. These observations are again different from results reported from measurements performed closer to BB sources in the Amazonian region, with SSA being higher at CHC than at the source regions. Reid et al. (1998) show that at Cuiaba, Porto Velho and Maraba, the SSA was around 0.80 from aircraft measurements during BB episodes. However, the authors report that the SSA values increase rapidly with time, i.e. from 0,85 to 0,90 in 1 or 2 days in this region (Reid et al., 1998

; Reid et al., 2005). The remote location of the Chacaltaya station thus explain high SSA values observed in the present study.

Figure (5b) shows the monthly variations of the Angström exponents. Even, AAE values are slightly lower than expected (between 1 and 2 according Russel et al., 2010), variations of AAE and SSAAE values exhibited typical seasonal variation~~values are well correlated to seasons~~. Lowest values of AAE are retrieved between December and March (mean AAE value of 0.8) and highest SSAAE values are retrieved during the same period (around 0.1). A seasonal variation of these intensive optical parameters shows that different sources of aerosol influence the CHC in different season. While AAE and SSAAE values show a significant seasonal variability, SAE values are more fluctuating. The highest SAE values are observed in April and September (up to 2) and persisting low values are seen between June and August. Ealo et al., (2016) used Angström coefficients to address the nature of aerosols. Applying their analysis technique, the seasonal evolution of AAE, SSAAE and SAE can be interpreted that urban emissions (low AAE values and high SSAAE and SAE values) contributes in the wet period in the La Paz region (from December to March) whereas dust particles mostly contribute in the dry and biomass-burning period (from April to November).

Figure (6a) shows the diurnal variations of aerosol particle optical properties averaged over the wet and dry seasons and BB period, and the diurnal variation of the standard deviation of the wind direction. For extensive optical parameters, a clear increase is observed starting around 08:00 in local time. This time evolution is observed for all seasons, as the result of the diurnal variation of the turbulent layer height described in Sect. 2.3. Optically scattering and absorbing particles emitted at ground level are mixed into the turbulent layer and reach the CHC altitude due to dynamic and convective effects of the atmosphere during daytime. Indeed, the variation of the atmospheric dynamics can be observed through the variation of the wind direction with significantly stronger turbulences between 08:00 and 12:00 and during all seasons.

From the diurnal variations one can also observe that not only the daytime optical properties exhibit pronounced seasonal variation, but also nighttime coefficients do, being influenced by the ~~SL~~SC ~~conditions~~ (Fig. 3). This confirms that emissions in the region have a clear influence on both ~~TL~~TC and ~~SL~~SC layers which can be measured at high altitude stations continuously.

The diurnal variation of the SSA shows a clear decrease at around 11:00, when only ~~TL~~TC particles are sampled at the station, indicating that ~~TL~~TC particles are relatively more absorbing compared to ~~SL~~SC particles. This observation can be explained by the local BC emission from traffic (Wiedensohler et al., 2018) and aged BB particles. Values can reach 0.90 a few hours after exhaust according Reid et al. (2005). Figure (A2~~1~~) allows to identify these urban influences of the in-situ measurements at CHC station through the difference of the AAE between workdays and Sundays.

Figure (6b) also shows hourly variations of the Angtsröm exponents for the three periods. A diurnal variation is observed mostly for SSAE values for the wet period, with an increase of more than 50% of SSAAE values during daytime compared to nighttime. As from extensive optical properties, these observations can be explained by the arrival of the ~~TL~~TC at CHC stations, with more local urban particles reaching the mountain station around 11:00.

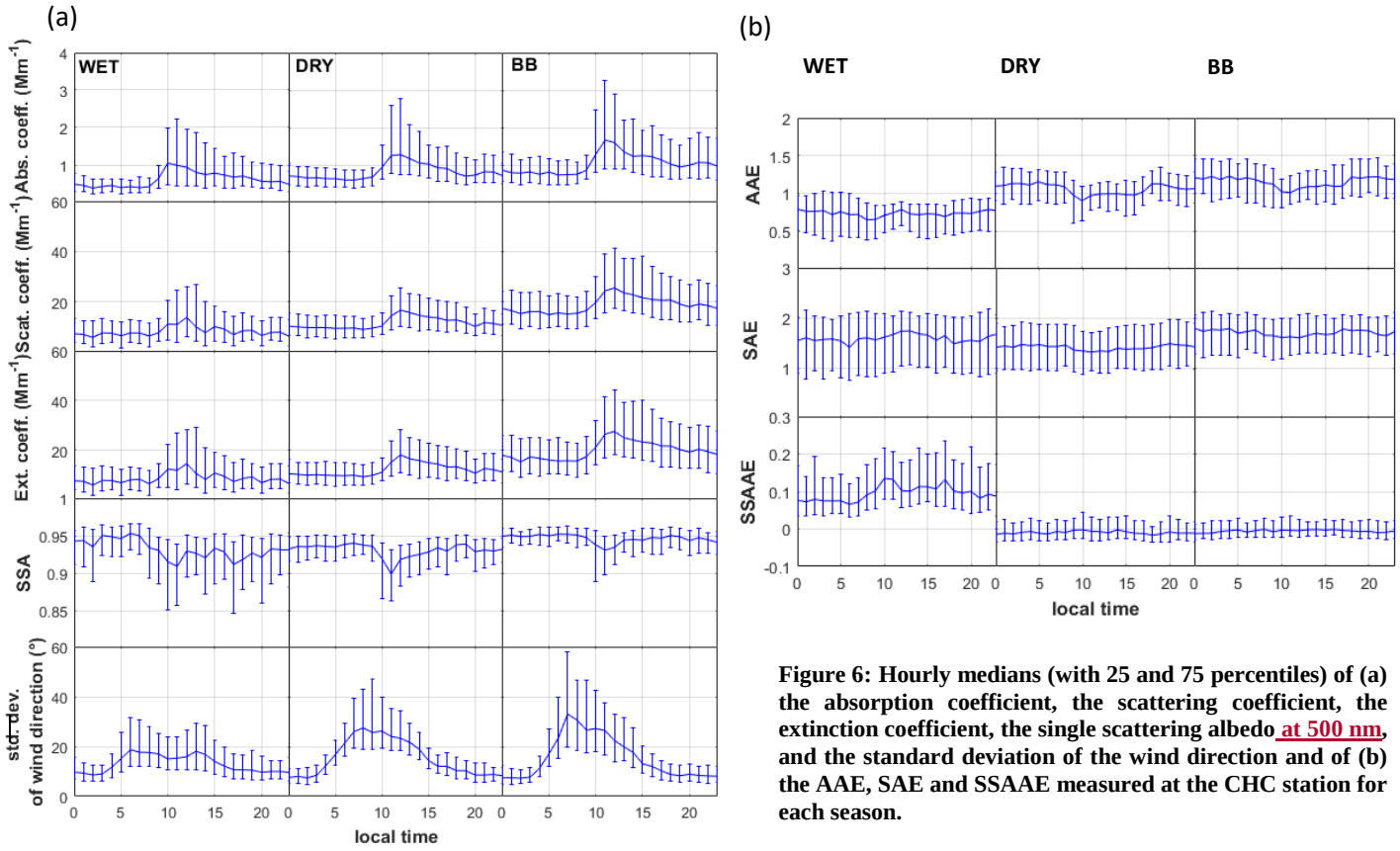

Figure 6: Hourly medians (with 25 and 75 percentiles) of (a) the absorption coefficient, the scattering coefficient, the extinction coefficient, the single scattering albedo at 500 nm, and the standard deviation of the wind direction and of (b) the AAE, SAE and SSAAE measured at the CHC station for each season.

3.3. Aerosol particle optical properties in stable and turbulent layer conditions

Using the method explained in Sect. 2.3, it is possible to characterize ~~SL~~SC and ~~TL~~TC optical properties separately. Median optical properties for each atmospheric ~~layer~~condition (~~TL~~TC and ~~SL~~SC) are presented Fig. (7) for each season (Wet, Dry and BB).

The optical properties of the particles sampled in the ~~TL~~TC are different from the ones sampled in the ~~SL~~SC ~~than the SL~~, with 1.49 times higher scattering coefficients, 1.94 times higher absorption coefficients, and 1.55 times higher extinction coefficients. We observe that the difference between ~~TL~~TC and ~~SL~~SC is highest during the wet season and lowest during the dry season. Indeed, the mean ~~TL~~TC to ~~SL~~SC ratio of extinction coefficients is 1.71 during the wet season, while it is only 1.49 during the dry season, and 1.44 during the BB period. These lower ~~TL~~TC to ~~SL~~SC ratios indicate that the ~~SL~~SC particles are more influenced by ~~TL~~TC intrusions during the dry season and the BB period than during the wet season.

These results also show that emissions from the Amazonian basin have important influence on the whole atmospheric column and at the regional scale. Indeed, both ~~SL~~SC and ~~TL~~TC ~~layers~~ present higher extinction coefficients during the BB period than the dry season (around 2 times higher). Same observations can be made for scattering and absorption coefficients.

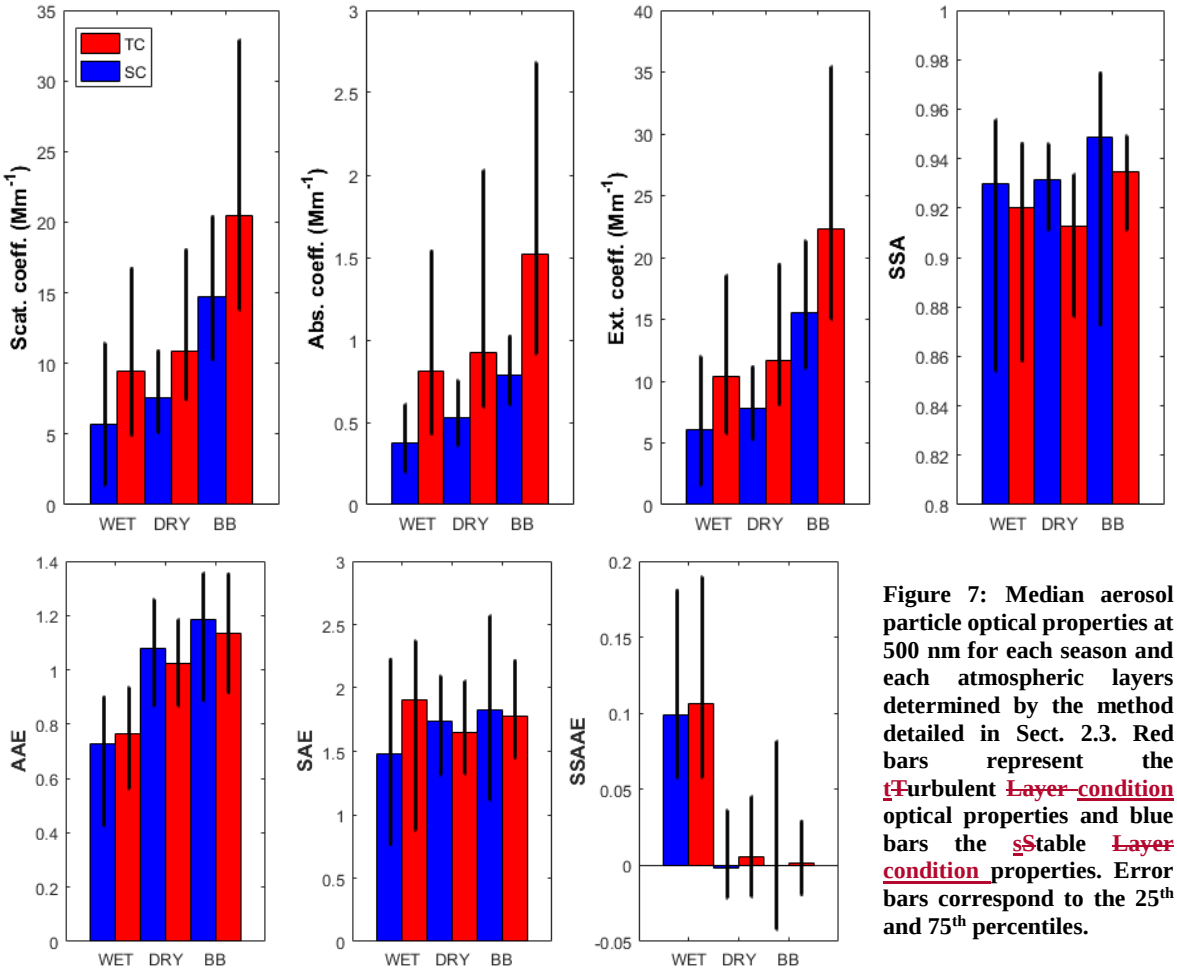

Figure 7: Median aerosol particle optical properties at 500 nm for each season and each atmospheric layers determined by the method detailed in Sect. 2.3. Red bars represent the t~~T~~urbulent ~~Layer~~ condition optical properties and blue bars the s~~S~~table ~~Layer~~ condition properties. Error bars correspond to the 25th and 75th percentiles.

The SSA values do not show a strong contrast between the ~~SL~~SC and the ~~TL~~TC although lower values are systematically observed in the ~~TL~~TC compared to the ~~SL~~SC (0.93, 0.93 and 0.95 during wet, dry and BB seasons respectively in the ~~SL~~SC ~~layer~~, and 0.92, 0.91 and 0.93 in the ~~TL~~TC ~~layer~~). As discussed by Reid et al. (2005), ~~SL~~SC aerosol particles are aged longer and transported farther than ~~TL~~TC particles due to less scavenging effects. The long transport modifies their optical properties to slightly increase the SSA. However, the small SSA difference between ~~TL~~TC and ~~SL~~SC indicates that the nature of the aerosol is actually similar between the ~~TL~~TC and ~~SL~~SC for a given season. As shown previously, the AAE increases in the dry and BB seasons, probably due to dust transport and to BB emissions. The contribution of dust is consistent with the drastic difference in SSAAE between wet season on one side and dry and BB seasons on the other. Not only SSA values, but also AAE, SAE and SSAAE values show weak ~~TL~~TC/~~SL~~SC contrast. This again illustrates that ageing processes of air masses into the full troposphere which homogenize their properties with time after emission.

3.4. Influences of air mass type on aerosol particle optical properties

The separation of air mass types into clusters allows us to analyze the influence of the different sources surrounding the station on their aerosol particle optical properties. The seasonal variability of aerosol particle optical properties may be attributed to a seasonal variability in the air mass types arriving at the station. As shown Fig. (4), air masses coming from the North-West (Clusters APO) dominates during the dry season, whereas air masses are from the East of the station. (Cluster NA and SA) plays a major role during the wet season. Figure (8) shows ~~TL~~TC and

~~SL~~SC optical properties. For each cluster and each season, the left bar indicates the ~~TL~~TC property, and the right bar the ~~SL~~SC property.

Figure 8: Aerosol particle optical properties from Chacaltaya measurements from 2012 to 2015 at 500 nm for TC~~L~~ (left bar), and SC~~L~~ (right bar) layers for each cluster and the three periods.

A strong air mass type dependence of the aerosol optical properties is found during the wet season. The highest extinction coefficients are found within air masses originating from the urban area of La Paz / El Alto (LP in green) with a median value of 13 Mm^{-1}. This value is significantly larger than other air-masses, which remains at less than 7 Mm^{-1}. The exceptionally high extinction coefficient can be mainly due to particle emissions from traffic in La Paz (Wiedensohler et al., 2018), despite the effect of wet deposition during this period. The lowest SSA are measured during the wet period, mainly within the NA air masses. This may be explained by important heating activities from the ~~Zongo Valley~~Yungas region, on the North-East slope of Cordillera Real at this period. Due to the wet deposition, aerosol particle life-times ~~are~~ is significantly decreased and the main part of aerosol particle optical measurements at CHC is from low altitudes (~~TL~~TC). Indeed, median ~~TL~~TC extinction coefficients are from 10% (for APO) to 200% (for NA) higher than values in the ~~SL~~SC.

During the dry season, extensive optical properties are larger than during the wet season for all clusters except for the cluster from the urban area of La Paz / El Alto (LP). The extinction coefficients are by more than 50% larger, with median values around 10 ± 2 Mm^{-1}. The soar of the extensive optical properties is due to low wet deposition rate during the dry season that extends aerosol lifetime. The extended aerosol lifetime allows local emissions to reach the in-situ station.

A further clear increase of all extensive optical properties are observed during the BB period. Extinction coefficients increase by 42% (LP) to 203% (NA). The cluster analysis shows that BB events impact atmospheric properties regionally influencing all clusters. However, higher increases are observed for air masses coming from the East (more than 80% higher for NA, SA, LP and NES) compared to direction from the West (45% to 70% higher), directly linked to intensive anthropogenic activities in the Amazonian Basin during this period. During extreme events, average extinction coefficients at CHC measurements can reach 247 Mm^{-1} (for NA). ~~, closer to the observations near BB sources (Husar et al., 2000).~~ A strong influence of BB emissions appears in ~~TL~~TC measurements with extinction values more than 160% higher than during the dry season, but a significant increase is also observed in the ~~SL~~SC measurements (around 110% higher to dry season for North-East air masses).

In addition to the classification of air masses into different clusters, we further classify aerosol particle types from their optical properties to characterize the influence of the different sources in this region.

Figure (9) shows the correlation of the Ångström exponents for absorption (AAE), scattering (SAE) and Single Scattering Albedo (SSAAE), for each season (symbols), each cluster (colors) and each tropospheric ~~layer~~conditions~~s~~ (filled marker for the ~~TL~~TC and un-filled markers for the ~~SL~~SC).

As shown in Fig. 5, low AAE values, especially during the wet season, can be explained by important reduction of dust and less biomass burning particles due to more efficient removal. ~~the high variability of aerosol loading from aethalometer measurements. In these conditions, aethalometer calibration may be impacted. However, AAE variations between season and clusters, especially during the dry season and the BB period, can be fully analysed.~~

As observed previously, Fig. (9) demonstrates that the wet season (diamonds) in this region is mainly influenced by a different source from the wet and the dry season. Thus, the wet season presents positive SSAAE and AAE close or lower than 0.9, while dry season and BB period present SSAAE close to 0 and AAE higher than 0.9. A linear relationship between AAE and SSAAE values is observed and ~~These values~~ illustrates that mainly urban emissions drive aerosol particle properties during the wet period, and that mainly dust emissions drive aerosol particle properties during the dry season and the BB period. Indeed, the large covering of arid surfaces on the Altiplano (West of the CHC station) presents an important source of dust. This result also indicates that whatever the air mass type, and the atmospheric ~~layer~~condition, ground emissions are influencing the optical properties of the whole atmospheric column and at a regional scale. In addition to dust emissions, BB period also demonstrates a significant contribution of BB combustion particles with higher median AAE values than during the dry season. Except for the NES cluster (West side of the Bolivian cordillera), AAE values are retrieved between 1.1 and 1.3 during BB period and between 0.9 and 1.1 during the dry season.

Even though there are dominant aerosol sources for each season as demonstrated in Fig. (8), the scatter plots of Ångström exponents in Fig. (9) provide additional insights into air mass origins. During the dry season, the scatterplot of AAE and SAE shows an important contribution of urban emissions in addition to the dominant dust aerosol. For some clusters, characteristics of urban emission is observed with AAE close to 1 and SAE higher than 1.4 for some clusters. During the BB period, a strong ~~TL~~TC/~~SL~~SC dependence is seen for La Paz / El Alto air masses (cluster LP). The AAE value for ~~TL~~TC ~~condition~~ indicates urban pollution effects (AAE below 1.1) whereas the AAE for ~~SL~~SC ~~conditions~~ shows an influence of BB emissions (AAE close to 1.3). A similar ~~SL~~SC dependence can also be observed for NA and APO clusters. Because AAE values are powerful tracers to separate urban and BB influences on aerosol particle optical properties, the ~~TL~~TC/~~SL~~SC dependence clearly demonstrates the influence of Amazonian biomass-burning on Chacaltaya in-situ measurements during the BB period within the ~~SL~~SC. Because BB particles are mainly emitt~~i~~ed from the East part of the Bolivian Cordillera, NES air masses are less influenced by these sources and present the lowest AAE values during the BB period.

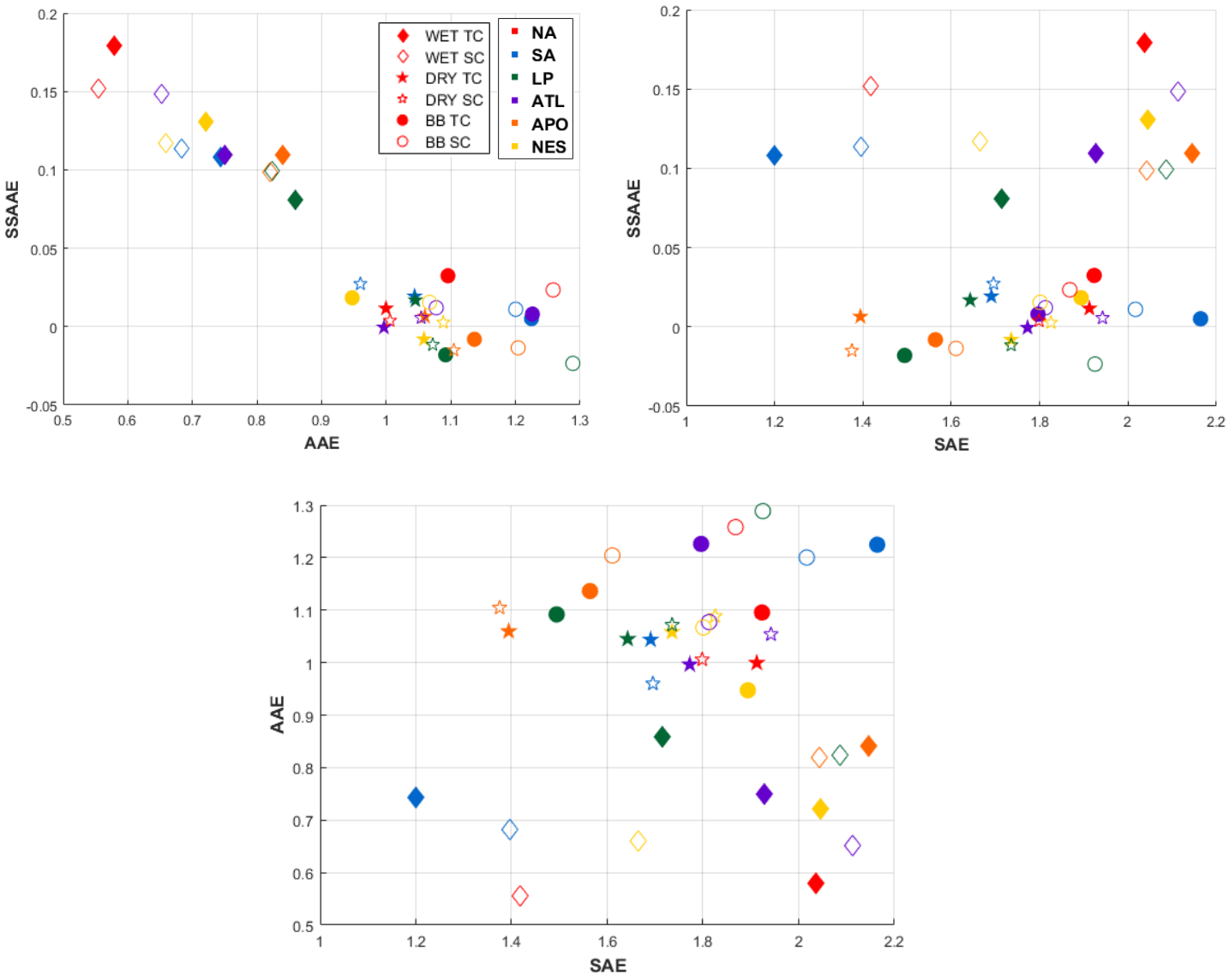

Figure 9: Wavelength dependence of optical properties measured at Chacaltaya station for each cluster (colors) and each season (markers) as parametrized by Ångström exponents. Diamonds correspond to median values during the WET period, stars correspond to the DRY period and circles correspond to the BB period.

The distribution of SAE is more spread, and the value depends on ~~layers~~atmospheric conditions, clusters and seasons. ~~As analysed previously~~In addition to urban influences, during the BB period and the wet season, LP air masses are also affected by dust particles, ~~less influenced by urban particles~~ especially in the ~~TL~~TC, ~~than in the SL~~ with ~~signifantly~~ lower SAE values ~~in the TL~~. The opposite is observed from NA air masses. While the main influence in these two air masses remains from urban emissions, it can be noticed that the lower part of the atmosphere (~~TL~~TC) in LP air masses are more affected by local dust particles than at the higer part of the atmosphere (~~SL~~SC). In NA cases, also observed for APO air masses, ~~SL~~SC measurements are less influenced by urban particles due to longer distance between CHC station and urban emissions than in LP cases.

Cluster	season	SAE	AAE	SSAAE	Aerosol types
NA	WET	2,04 (1,42)	0,58 (0,56)	0,18 (0,15)	urban (dust/urban)
	DRY	1,91 (1,80)	1,00 (1,01)	0,01 (0,004)	urban (dust)
	BB	1,92 (1,87)	1,10 (1,26)	0,03 (0,02)	dust/BB (dust/BB)
SA	WET	1,2 (1,40)	0,74 (0,68)	0,11 (0,11)	urban (urban)
	DRY	1,69 (1,70)	1,04 (0,96)	0,02 (0,03)	dust (dust)

	BB	2,16 (2,02)	1,23 (1,20)	0,005 (0,01)	BB (BB)
LP	WET	1,71 (2,09)	0,86 (0,82)	0,08 (0,10)	urban (urban)
	DRY	1,64 (1,74)	1,05 (1,07)	0,02 (-0,01)	urban (dust/urban)
	BB	1,49 (1,93)	1,09 (1,29)	-0,02 (-0,02)	dust (dust/BB)
ATL	WET	1,93 (2,11)	0,75 (0,65)	0,11 (0,15)	urban (urban)
	DRY	1,77 (1,94)	1,00 (1,05)	-0,001 (0,006)	dust (dust/urban)
	BB	1,80 (1,81)	1,23 (1,08)	0,008 (0,01)	dust/BB (urban)
APO	WET	2,15 (2,04)	0,84 (0,82)	0,11 (0,10)	urban (urban)
	DRY	1,39 (1,38)	1,06 (1,10)	0,006 (-0,02)	dust (dust)
	BB	1,56 (1,61)	1,14 (1,20)	-0,008 (-0,01)	dust/BB (dust/BB)
NES	WET	2,05 (1,67)	0,72 (0,66)	0,13 (0,12)	urban (urban)
	DRY	1,74 (1,83)	1,06 (1,09)	-0,008 (0,003)	dust/urban (dust)
	BB	1,89 (1,80)	0,95 (1,07)	0,002 (0,02)	dust/urban (urban)

Table 2: Median aerosol Angström exponents of turbulent condition (stable condition) for each cluster and seasons measured at the CHC station and resulting aerosol types.

Table 2 summarizes the median Angström exponents measured at the CHC station for turbulent conditions (stable conditions in parenthesis). According to these values and as discussed above, aerosol types for the turbulent conditions (and stable conditions in parenthesis) are given.

Conclusions

~~This study reports on the variability of aerosol particle optical properties at a high altitude site in the Bolivian cordillera (Chacaltaya, 5240 m a.s.l.).~~ Chacaltaya station is currently the unique high-altitude atmospheric observatory in the Andes. The location of the station allows to sample air masses of different types (mainly urban, biomass-burning and dust particles). Measurements have been run over a long-term period at a high temporal resolution and a large set of instruments. This study reports on the impact of several aerosol sources in South-America through the variability of aerosol particle optical properties. ~~The study~~We show~~s~~ that the ~~Chacaltaya~~ Central Andean region (cordillera Real) is characterized by median annual values of absorption, scattering and extinction coefficients of 0.74, 12.14 and 12.96 Mm^{-1} respectively. Results also show the effect of the two main seasons, a dry and a wet season, on aerosol particle optical properties characteristic of different source influences. Diurnal variations are also observed due to Atmospheric Boundary Layer dynamics influencing this high altitude location ~~of the Chacaltaya in-situ station~~.

The topography of the surrounding region also gives unique opportunities to sample aerosol particle optical properties within different atmospheric ~~layer~~conditions. For each season, stable ~~layer~~conditions (~~SL~~SC) ~~conditions~~ have been identified in contrast to turbulent conditions ~~layer~~ (~~TL~~TC) ~~conditions~~ using the standard deviation of the wind direction. Even ~~TL~~TC is usually attributed to mixing ~~or residual~~ layer~~s~~, ~~SL~~SC can be undoubtedly attributed to free tropospheric ~~layers~~or residual layers.

Every year, from July to November, this region is influenced by important biomass-burning activities at the regional scale. The present study clearly demonstrates the regional impacts of these activities. Results show higher scattering and absorption coefficients during the BB period (44% to 144% increase compared to the dry season) that can be observed in all tropospheric layers. The present study has hence demonstrated that BB particles are efficiently transported to the higher part of the troposphere (Stable conditions) and over long distances (more than 300 km long). However, differences in the~~of~~ optical properties between different air mass types are less pronounced in the ~~SL~~SC than in the ~~TL~~TC, which can be mainly explained by the longer life time of the aerosol particles within the higher troposphere.

One of the main aerosol sources in the Bolivian plateau is t~~T~~he urban area of La Paz / El Alto. It contributes significantly to optical properties of the atmosphere due to important traffic emissions and industries (Wiedensohler et al., 2018). In addition to BB activities, the urban area with 1.7 million inhabitants, located at 17

km south to the CHC station between 3200 and 4000 m a.s.l, was ~~also~~ found to contribute significantly to the optical characteristics of the aerosol particles sampled at CHC. The lowest single scattering albedo values (median of 0.85), attributed to incomplete combustion, was observed for back-trajectories from the urban area of La Paz / El Alto during the wet season, and the same air-mass has the highest extinction coefficient during the wet season. This~~A~~ strong signature of pollution aerosols is also ~~found in air masses originating from the La Paz - El Alto area, witnessed~~highlighted by the wavelength dependence of the absorption ~~(~~Angström exponent (AAE) both ~~for~~ in ~~TL~~TC and ~~SL~~SC ~~atmospheric layers~~.

Finally, the arid plateau of the region has also demonstrated regional impact. ~~to contribute to the aerosol particle load at the Chacaltaya station.~~ In addition to urban and BB influences, t~~T~~he wavelength dependence of the single scattering albedo (SSAAE) measured at CHC highlights a main dust influence during the entire dry season with SSAAE values close to 0. This influence is no longer observed during the wet season due to particle scavenging and less dust uprising due to wet soils.

Aerosol type	SAE	AAE	SSAAE
Dust	-	> 0,9	[-0,05 ; 0,05]
Urban pollution	> 1,4	< 0,9	> 0,05
Biomass burning	-	> 1,1	[-0,05 ; 0,05]

Table 3: Updated Angström exponent values expected for aerosol types at the CHC station.

A new Angtsröm exponent classification can then be defined for measurement at the CHC station and is reported Table 3. Thresholds are close to the ones proposed by previous works (Dubovik et al., 2002 ; Collaud Coen et al., 2004 ; Clarke et al., 2007 ; Russel et al., 2010) but adapted to CHC's instruments and particular atmospheric conditions.

The in-situ measurements of the high-altitude station of Chacaltaya provide useful information on the different aerosol sources in this region ~~in both the TL and SL layers~~. Thus, they can be used to validate satellite products as Cloud Aerosol Lidar and Infrared Pathfinder Satellite Observations (CALIPSO) LIDAR measurements of the vertical aerosol profiles, when chosen at the adequate time of the day. We also found that most aerosol intrinsic properties were very similar over the whole atmospheric column ~~in both layers~~, thus indicating that those can also be used to validate Moderate Resolution Imaging Spectroradiometer (MODIS) measurements of columnar aerosol particle optical depth over the bright region at high elevation.

Author contributions: P.G., I.M., and F.V., with the help of the UMSA, carried out the measurements at the station. M.A., K.S., A.W. and P.L. supervised the project. D.A. and F.V. did trajectory analyses and I.M. developed the method to discriminate stable and turbulent conditions. A.C wrote the manuscript with the help of D.A. R.K, G.M, and T.M., brought instrumental instructions to convert and correct measurements. N. M., M.P. and K.W. helped shape the research and analysis. All authors discussed the results and contributed to the final manuscript.

Acknowledgements. Day-to-day operations at CHC station are under the responsibility and support of UMSA through the Institute for Physics Research (Laboratorio de fisica de la Atmosfera).
This work was also accomplished in the frame of the project ACTRIS-2 (Aerosols, Clouds, and Trace gases Research InfraStructure) under the European Union – Research Infrastructure Action in the frame of the H2020 program for "Integrating and opening existing national and regional research infrastructures of European interest" under Grant Agreement N°654109.
We acknowledge the support from IRD (Institut de Recherche pour le Développement) under Jeune Equipe program CHARME awarded to LFA, by Labex OSUG@2020 (Investissements d'avenir – ANR10 LABX56) and INSU-CNRS under the Service National d'observation programme CLAP and ACTRIS-FR.
We gratefully acknowledge Souichiro Hioki for his help on english corrections and proofreadings.

Appendix:

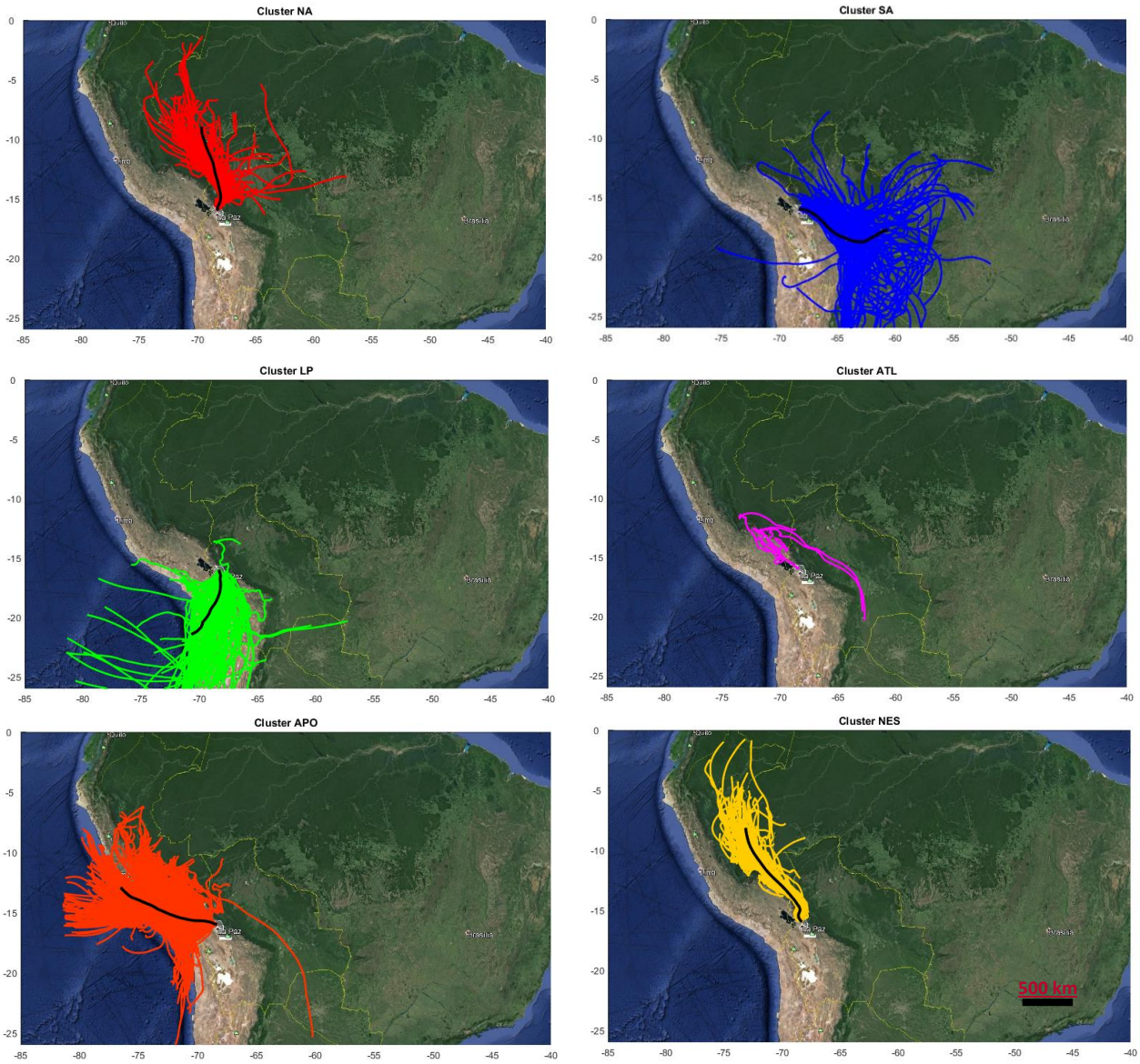

Figure A1: Selected 96-hours back-trajectories for the six clusters obtained from the Borge et al. (2007) method. The black line corresponds to the main back-trajectory.

For each hour of the period of the study, nine back-trajectories have been used to describe the mean influence at Chacaltaya station. The nine BTs start within a square of 2 km by 2 km around the station. The mean BT has been calculated from these nine BTs and generated every hour from January 2012 to December 2015. Clusters are defined according the Borge et al. (2017) methods using a two-stage technique (based on the non-hierarchical K-means algorithm). The Borge et al. (2007) method allows to attribute to each mean BT a fraction of each cluster according to their time residence into the cluster and their distance from the CHC station. Hence, BTs are sorted according to their representativeness in each cluster. The first 10% of them are used in the present study and are reported in Fig. (A1).

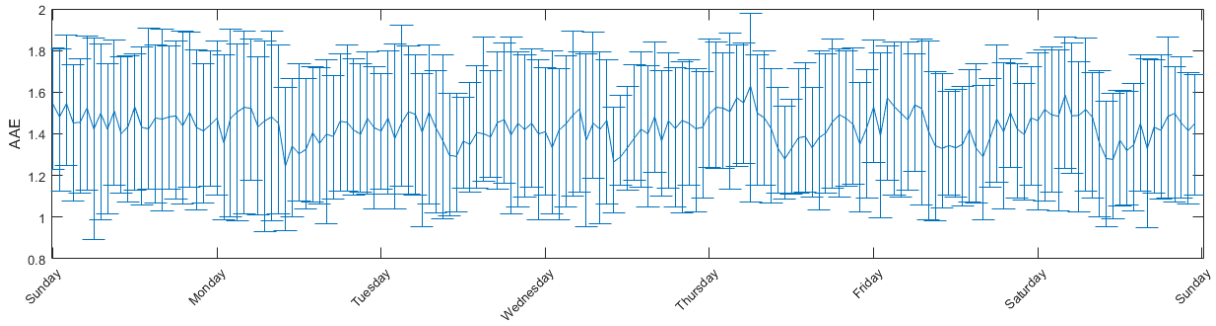

Figure A2~~1~~: Weekly variation of the Aerosol Angström Exponent (AAE) for the whole~~all~~ dataset from 2012 to 2015. The medians ~~are represented in addition to~~ and their 25th and 75th percentiles from Sundays to Saturdays are repsresented.

The weekly variation of the Absorption Angström Exponent (AAE) is shown in Fig. (A2~~1~~) for the four years' dataset. This representation of in-situ measurements at Chacaltaya station allows a~~to~~ better discrimina~~t~~tion~~e~~ of
565 anthropogenic influence on the aerosol optical properties.

Net decrease of the AAE is observed for every working day at about 10:00 - with median values of 1.2 in contrast to around 1.5 in the beginning and the end of the day – whereas Sundays clearly show constant (±0.05) values of AAE for the all day. These observations show that aerosol concentrations measured on Chacaltaya greatly depends on the activities in the urbanized area below the station.

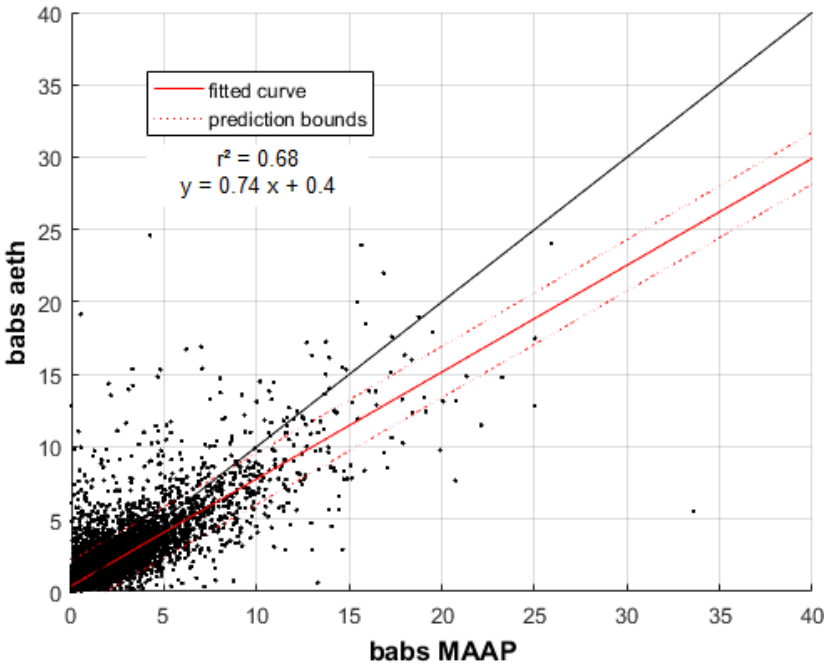

Figure A3~~2~~: Comparison of absorption coefficients measured at 635 nm according aethalometer and MAAP measurements from the CHC dataset between 2012 and 2014. Black line corresponds to the 1 to 1 fit.

570 Figure (A3~~2~~) shows comparison of absorption coefficients at 635 nm measured by the aethalometer and the MAAP at CHC station from 2012 to 2014. Because MAAP measurements can measure the aerosol particle absorption coefficient with a better accuracy (Saturno et al., 2017), this study validates the correction method by Weingartner et al. (2003) that is applied to the aethalometer measurements as preconized by ACTRIS (Müller et al., 2011a ; Drinovec et al., 2015).

References:

Artaxo, P., V. Rizzo, L., F. Brito, J., J. Barbosa, H. M., Arana, A., T. Sena, E., G. Cirino, G., Bastos, W., T. Martin, S. and O. Andreae, M.: Atmospheric aerosols in Amazonia and land use change: from natural biogenic to biomass-burning conditions, Faraday Discuss., 165(0), 203–235, doi:10.1039/C3FD00052D, 2013.

Borge, R., Lumbreras, J., Vardoulakis, S., Kassomenos, P. and Rodríguez, E.: Analysis of long-range transport influences on urban PM 10 using two-stage atmospheric trajectory clusters, Atmos. Environ., 41(21), 4434–4450, 2007.

Boucher, O., Randall, D., Artaxo, P., Bretherton, C., Feingold, G.,Forster, P., Kerminen, V.-M., Kondo, Y., Liao, H., Lohmann, U.,Rasch, P., Satheesh, S., Sherwood, S., Stevens, B., and Zhang,X.: Clouds and Aerosols, book section 7, 571–658, CambridgeUniversity Press, Cambridge, UK and New York, NY, USA,https://doi.org/10.1017/CBO9781107415324.016, 2013.

Bourgeois, Q., Ekman, A. M. L. and Krejci, R.: Aerosol transport over the Andes from the Amazon Basin to the remote Pacific Ocean: A multiyear CALIOP assessment, J. Geophys. Res. Atmospheres, 120(16), 2015JD023254, doi:10.1002/2015JD023254, 2015.

Carmona-Moreno, C., Belward, A., Malingreau, J.-P., Hartley, A., Garcia-Alegre, M., Antonovskiy, M., Buchshtaber, V. and Pivovarov, V.: Characterizing interannual variations in global fire calendar using data from Earth observing satellites, Global Change Biology, 11(9), 1537–1555, 2005.

Charlson, R. J., Schwartz, S. E., Hales, J. M., Cess, R. D.,Coakley, J. A., Hansen, J. E., and Hofmann, D. J.: ClimateForcing by Anthropogenic Aerosols, Science, 255, 423–430, https://doi.org/10.1126/science.255.5043.423, 1992.

Clarke, A., McNaughton, C., Kapustin, V., Shinozuka, Y., Howell, S., Dibb, J., Zhou, J., Anderson, B., Brekhovskikh, V., Turner, H. and Pinkerton, M.: Biomass burning and pollution aerosol over North America: Organic components and their influence on spectral optical properties and humidification response, J. Geophys. Res. Atmospheres, 112(D12), D12S18, doi:10.1029/2006JD007777, 2007.

Collaud Coen, M., E. Weingartner, D. Schaub, C. Hueglin, C. Corrigan, S. Henning, M. Schwikowski, and Urs Baltensperger. « Saharan dust events at the Jungfraujoch: detection by wavelength dependence of the single scattering albedo and first climatology analysis ». Atmospheric Chem. Phys. 4, no 11/12 : 2465–2480. 2004.

Collaud Coen, M., Weingartner, E., Apituley, A., Ceburnis, D., Fierz-Schmidhauser, R., Flentje, H., Henzing, J. S., Jennings, S. G., Moerman, M., Petzold, A., Schmid, O. and Baltensperger, U.: Minimizing light absorption measurement artifacts of the Aethalometer: evaluation of five correction algorithms, Atmospheric Measurement Techniques, 3(2), 457–474, doi:10.5194/amt-3-457-2010, 2010.

Drinovec, L., Močnik, G., Zotter, P., Prévôt, A. S. H., Ruckstuhl, C., Coz, E., Rupakheti, M., Sciare, J., Müller, T., Wiedensohler, A. and Hansen, A. D. A.: The "dual-spot" Aethalometer: an improved measurement of aerosol black carbon with real-time loading compensation, Atmospheric Meas. Tech., 8(5), 1965–1979, doi:10.5194/amt-8-1965-2015, 2015.

Dubovik, O. and King, M. D.: A flexible inversion algorithm for retrieval of aerosol optical properties from Sun and sky radiance measurements, J. Geophys. Res. Atmospheres, 105, 20673–20696, 2000.

Dubovik, O., Smirnov, A., Holben, B. N., King, M. D., Kaufman, Y. J., Eck, T. F. and Slutsker, I.: Accuracy assessments of aerosol optical properties retrieved from Aerosol Robotic Network (AERONET) Sun and sky radiance measurements, J. Geophys. Res., 105(D8), 9791–9806, doi:10.1029/2000JD900040, 2000.

Dubovik, O., Holben, B., Eck, T. F., Smirnov, A., Kaufman, Y. J., King, M. D., Tanre, D. and Slutsker, I.: Variability of absorption and optical properties of key aerosol types observed in worldwide locations, J. Atmospheric Sci., 59, 590–608, doi:Review, 2002.

Ealo, M., Alastuey, A., Ripoll, A., Pérez, N., Minguillón, M. C., Querol, X. and Pandolfi, M.: Detection of Saharan dust and biomass-burning events using near-real-time intensive aerosol optical properties in the north-western Mediterranean, Atmospheric Chem. Phys., 16(19), 12567–12586, 2016.

Giglio, L., Randerson, J. T. and van der Werf, G. R.: Analysis of daily, monthly, and annual burned area using the fourth-generation global fire emissions database (GFED4), Journal of Geophysical Research: Biogeosciences, 118(1), 317–328, 2013.

Hamburger, T., Matisāns, M., Tunved, P., Ström, J., Calderon, S., Hoffmann, P., Hochschild, G., Gross, J., Schmeissner, T. and Wiedensohler, A.: Long-term in situ observations of biomass-burning aerosol at a high altitude station in Venezuela–sources, impacts and interannual variability, Atmospheric Chem. Phys., 13(19), 9837–9853, 2013.

Hansen, A. D. A., Rosen, H., and Novakov, T.: Real-time measurement of the aerosol absoprtion-coefficient of aerosol particles, Appl. Opt., 21, 3060–3062, doi:10.1364/AO.21.003060, 1982.

Hansen, J., Sato, M., and Ruedy, R.: Radiative forcing and climate response, J. Geophys. Res.- Ser.-, 102, 6831–6864, 1997.

Husar, R. B., Husar, J. D. and Martin, L.: Distribution of continental surface aerosol extinction based on visual range data, Atmos. Environ., 34(29–30), 5067–5078, doi:10.1016/S1352-2310(00)00324-1, 2000.

IPCC. Climate change 2013 : The physical science basis. Cambridge University Press. 2013

Krejci, R., Ström, J., de Reus, M., Hoor, P., Williams, J., Fischer, H. and Hansson, H.-C.: Evolution of aerosol properties over the rain forest in Surinam, South America, observed from aircraft during the LBA-CLAIRE 98 experiment, J. Geophys. Res. Atmospheres, 108(D18), 4561, doi:10.1029/2001JD001375, 2003.

Kuniyal, J. C. and Guleria, R.: The current state of aerosol-radiation interactions: A mini review, J. Aerosol Sci., 130, doi:10.1016/j.jaerosci.2018.12.010, 2018.

Liousse, C., Cachier, H. and Jennings, S. G.: Optical and thermal measurements of black carbon aerosol content in different environments: Variation of the specific attenuation cross-section, sigma (σ), Atmospheric Environment. Part A. General Topics, 27(8), 1203–1211, 1993.

Marcq, S., Laj, P., Roger, J. C., Villani, P., Sellegri, K., Bonasoni, P., Marinoni, A., Cristofanelli, P., Verza, G. P. and Bergin, M.: Aerosol optical properties and radiative forcing in the high Himalaya based on measurements at the Nepal Climate Observatory-Pyramid site (5079 m a.s.l.), Atmos Chem Phys, 10(13), 5859–5872, doi:10.5194/acp-10-5859-2010, 2010.

Marenco, F., Johnson, B., Langridge, J. M., Mulcahy, J., Benedetti, A., Remy, S., Jones, L., Szpek, K., Haywood, J., Longo, K. and Artaxo, P.: On the vertical distribution of smoke in the Amazonian atmosphere during the dry season, Atmospheric Chem. Phys., 16(4), 2155–2174, doi:10.5194/acp-16-2155-2016, 2016.

Martin, S. T., Andreae, M. O., Artaxo, P., Baumgardner, D., Chen, Q., Goldstein, A. H., Guenther, A., Heald, C. L., Mayol-Bracero, O. L., McMurry, P. H., Pauliquevis, T., Pöschl, U., Prather, K. A., Roberts, G. C., Saleska, S. R., Silva Dias, M. A., Spracklen, D. V., Swietlicki, E. and Trebs, I.: Sources and properties of Amazonian aerosol particles, Rev. Geophys., 48(2), RG2002, doi:10.1029/2008RG000280, 2010.

Moosmüller, H. and Chakrabarty, R. K.: Simple analytical relationships between Angström coefficients of aerosol extinction, scattering, absorption, and single scattering albedo, Atmospheric Chem. Phys., 11(20), 10677–10680, 2011.

Müller, T., Henzing, J. S., de Leeuw, G., Wiedensohler, A., Alastuey, A., Angelov, H., Bizjak, M., Collaud Coen, M., Engström, J. E., Gruening, C., Hillamo, R., Hoffer, A., Imre, K., Ivanow, P., Jennings, G., Sun, J. Y., Kalivitis, N., Karlsson, H., Komppula, M., Laj, P., Li, S.-M., Lunder, C., Marinoni, A., Martins dos Santos, S., Moerman, M., Nowak, A., Ogren, J. A., Petzold, A., Pichon, J. M., Rodriquez, S., Sharma, S., Sheridan, P. J., Teinilä, K., Tuch, T., Viana, M., Virkkula, A., Weingartner, E., Wilhelm, R. and Wang, Y. Q.: Characterization and intercomparison of aerosol absorption photometers: result of two intercomparison workshops, Atmospheric Meas. Tech., 4(2), 245–268, doi:10.5194/amt-4-245-2011, 2011a.

Müller, T., Laborde, M., Kassell, G. and Wiedensohler, A.: Design and performance of a three-wavelength LED-based total scatter and backscatter integrating nephelometer, Atmospheric Meas. Tech., 4(6), 1291–1303, doi:10.5194/amt-4-1291-2011, 2011b.

Myhre, G., Samset, B. H., Schulz, M., Balkanski, Y., Bauer, S., Berntsen, T. K., Bian, H., Bellouin, N., Chin, M., Diehl, T., Easter, R. C., Feichter, J., Ghan, S. J., Hauglustaine, D., Iversen, T., Kinne, S., Kirkevåg, A., Lamarque, J.-F., Lin, G., Liu, X., Lund, M. T., Luo, G., Ma, X., van Noije, T., Penner, J. E., Rasch, P. J., Ruiz, A., Seland, Ø., Skeie, R. B., Stier, P., Takemura, T., Tsigaridis, K., Wang, P., Wang, Z., Xu, L., Yu, H., Yu, F., Yoon, J.-H., Zhang, K., Zhang, H., and Zhou, C.: Radiative forcing of the direct aerosol effect from AeroCom Phase II simulations, Atmospheric Chem. Phys., 13, 1853-1877, https://doi.org/10.5194/acp-13-1853-2013, 2013.

Petzold, A. and Schönlinner, M.: Multi-angle absorption photometry--a new method for the measurement of aerosol light absorption and atmospheric black carbon, J. Aerosol Sci., 35, 421–441, doi:DOI: 10.1016/j.jaerosci.2003.09.005, 2004.

Procopio, A. S., Artaxo, P., Kaufman, Y. J., Remer, L. A., Schafer, J. S. and Holben, B. N.: Multiyear analysis of amazonian biomass-burning smoke radiative forcing of climate, Geophys. Res. Lett., 31(3), L03108, doi:10.1029/2003GL018646, 2004.

Rajesh, T. A. and Ramachandran, S.: Black carbon aerosol mass concentration, absorption and single scattering albedo from single and dual spot aethalometers: Radiative implications, Journal of Aerosol Science, 119, 77–90, 2018.

Reid, J. S., Hobbs, P. V., Ferek, R. J., Blake, D. R., Martins, J. V., Dunlap, M. R. and Liousse, C.: Physical, chemical, and optical properties of regional hazes dominated by smoke in Brazil, J. Geophys. Res. Atmospheres, 103(D24), 32059–32080, doi:10.1029/98JD00458, 1998.

Reid, J. S., Eck, T. F., Christopher, S. A., Koppmann, R., Dubovik, O., Eleuterio, D. P., Holben, B. N., Reid, E. A. and Zhang, J.: A review of biomass-burning emissions part III: intensive optical properties of biomass-burning particles, Atmospheric Chem. Phys., 5(3), 827–849, 2005.

Rose, C., Sellegri, K., Velarde, F., Moreno, I., Ramonet, M., Weinhold, K., Krejci, R., Ginot, P., Andrade, M. and Wiedensohler, A.: Frequent nucleation events at the high altitude station of Chacaltaya (5240 m asl), Bolivia, Atmos. Environ., 102, 18–29, 2015.

Rose, C., Sellegri, K., Moreno, I., Velarde, F., Ramonet, M., Weinhold, K., Krejci, R., Andrade, M., Wiedensohler, A. and Ginot, P.: CCN production by new particle formation in the free troposphere, Atmospheric Chemistry and Physics, 17(2), 1529–1541, 2017.

Russell, P. B., Bergstrom, R. W., Shinozuka, Y., Clarke, A. D., DeCarlo, P. F., Jimenez, J. L., Livingston, J. M., Redemann, J., Dubovik, O. and Strawa, A.: Absorption Angstrom Exponent in AERONET and related data as an indicator of aerosol composition, Atmospheric Chem. Phys., 10, 1155–1169, doi:10.5194/acp-10-1155-2010, 2010.

Rose, C., Sellegri, K., Moreno, I., Velarde, F., Ramonet, M., Weinhold, K., Krejci, R., Andrade, M., Wiedensohler, A. and Ginot, P.: CCN production by new particle formation in the free troposphere, Atmospheric Chem. Phys., 17(2), 1529–1541, 2017.

Samset, B. H., Myhre, G., Schulz, M., Balkanski, Y., Bauer, S., Berntsen, T. K., Bian, H., Bellouin, N., Diehl, T., Easter, R. C., Ghan, S. J., Iversen, T., Kinne, S., Kirkevåg, A., Lamarque, J.-F., Lin, G., Liu, X., Penner, J. E., Seland, Ø., Skeie, R. B., Stier, P., Takemura, T., Tsigaridis, K. and Zhang, K.: Black carbon vertical profiles strongly affect its radiative forcing uncertainty, Atmospheric Chem. Phys., 13(5), 2423–2434, doi:10.5194/acp-13-2423-2013, 2013.

Samset, B. H., Myhre, G., Herber, A., Kondo, Y., Li, S.-M., Moteki, N., Koike, M., Oshima, N., Schwarz, J. P., Balkanski, Y., Bauer, S. E., Bellouin, N., Berntsen, T. K., Bian, H., Chin, M., Diehl, T., Easter, R. C., Ghan, S. J., Iversen, T., Kirkevåg, A., Lamarque, J.-F., Lin, G., Liu, X., Penner, J. E., Schulz, M., Seland, Ø., Skeie, R. B., Stier, P., Takemura, T., Tsigaridis, K. and Zhang, K.: Modelled black carbon radiative forcing and atmospheric lifetime in AeroCom Phase II constrained by aircraft observations, Atmospheric Chem. Phys., 14(22), 12465–12477, doi:10.5194/acp-14-12465-2014, 2014.

Saturno, J., Pöhlker, C., Massabó, D., Brito, J., Carbone, S., Cheng, Y., Chi, X. and Ditas, F.: Comparison of different Aethalometer correction schemes and a reference multi-wavelength absorption technique for ambient aerosol data, Atmospheric Meas. Tech., 15, 2017.

Schafer, J. S., Eck, T. F., Holben, B. N., Artaxo, P. and Duarte, A. F.: Characterization of the optical properties of atmospheric aerosols in Amazônia from long-term AERONET monitoring (1993–1995 and 1999–2006), Journal of Geophysical Research: Atmospheres, 113(D4), doi:10.1029/2007JD009319, 2008.

Stein, A. F., Draxler, R. R., Rolph, G. D., Stunder, B. J. B., Cohen, M. D., and Ngan, F.: NOAA's HYSPLIT atmospheric transport and dispersion modeling system, B. Am. Meteorol. Soc., 96, 2059–2077, doi:10.1175/BAMS-D-14-00110.1, 2015.

Wiedensohler, A., Andrade, M., Weinhold, K., Müller, T., Birmili, W., Velarde, F., Moreno, I., Forno, R., Sanchez, M. F. and Laj, P.: Black carbon emission and transport mechanisms to the free troposphere at the La Paz/El Alto (Bolivia) metropolitan area based on the Day of Census (2012), Atmos. Environ., 194, 158–169, 2018.

Weingartner, E., Saathoff, H., Schnaiter, M., Streit, N., Bitnar, B. and Baltensperger, U.: Absorption of light by soot particles: determination of the absorption coefficient by means of aethalometers, J. Aerosol Sci., 34(10), 1445–1463, doi:10.1016/S0021-8502(03)00359-8, 2003.

Whiteman, C. D.: Mountain meteorology: fundamentals and applications, Oxford University Press., 2000.

WMO/GAW Aerosol Measurement Procedures, Guidelines and Recommendations 2nd Edition page 39, World Meteorological Organization, Geneva, 2016.

Yamartino, R. J.: A comparison of several “single-pass” estimators of the standard deviation of wind direction, J. Clim. Appl. Meteorol., 23(9), 1362–1366, 1984.

Anonymous Referee #2

Received and published: 11 August 2019

Authors would like to thank the reviewer for his/her interest in the work and the constructive suggestions. Corrections allow us to clarify the method used for clustering and highlight the main goals of the paper.

The atmospheric stability is used as a tracer to differentiate the atmospheric layers. As recommended, Stable Layer (SC) and Turbulent Layer (TL) are have been replaced by Stable Conditions (SC) and Turbulent Conditions (TC). This was also requested by other 2 reviewers.

In the following, we provide answers to the reviewer's comments and list the modifications made in the manuscript.

This work reviews the optical properties of aerosol sampled in a mainly free tropospheric site in Bolivia for a period that spans 4 years. The authors have performed a very comprehensive and thorough analysis of their results categorizing the optical properties of aerosol in the area based on the layer sampled (FT or PBL), based on source region and on seasons. The manuscript provides a rather complete picture of the aerosol optical properties of Chacaltaya with the only information missing is the composition of the measured particles. Even though, it is understood that such information (on composition) cannot be included in this work, a short summary would be more than welcome. I recommend that this work is published with only some minor additions which I list below.

Please add a table and summarize in a small paragraph what type of particles (dust,urban, ..etc) are expected to be sampled in each season, layer and source region based on the types of categorization performed in this work. This information is available, but scattered throughout the manuscript and if you compile into one small paragraph the reader will be greatly assisted in understanding your work.

Answer: Three tables have been added to the text which summarize information from the text. The Table 1 summarizes ranges of Angström exponent for the different aerosol types. Table 2 details the median values of the Angström exponent for each cluster, season and atmospheric stability. Table 3, on the conclusion, suggests a new Angtsröm exponent definition for the different aerosol types.

Modifications:

Aerosol type	SAE	AAE	SSAAE
Dust	Close to 1	Close to 1	Below 0
Urban pollution	Close to 2	Close to 1	Higher than 0
Biomass burning		Close to 2,1	

Table 1: Expected aerosol type and their optical properties for each cluster according season and atmospheric stability.

Cluster	season	SAE	AAE	SSAAE	Aerosol types
NA	WET	2,04 (1,42)	0,58 (0,56)	0,18 (0,15)	urban (dust/urban)
	DRY	1,91 (1,80)	1,00 (1,01)	0,01 (0,004)	urban (dust)
	BB	1,92 (1,87)	1,10 (1,26)	0,03 (0,02)	dust/BB (dust/BB)
SA	WET	1,2 (1,40)	0,74 (0,68)	0,11 (0,11)	urban (urban)
	DRY	1,69 (1,70)	1,04 (0,96)	0,02 (0,03)	dust (dust)
	BB	2,16 (2,02)	1,23 (1,20)	0,005 (0,01)	BB (BB)
LP	WET	1,71 (2,09)	0,86 (0,82)	0,08 (0,10)	urban (urban)
	DRY	1,64 (1,74)	1,05 (1,07)	0,02 (-0,01)	urban (dust/urban)
	BB	1,49 (1,93)	1,09 (1,29)	-0,02 (-0,02)	dust (dust/BB)
ATL	WET	1,93 (2,11)	0,75 (0,65)	0,11 (0,15)	urban (urban)
	DRY	1,77 (1,94)	1,00 (1,05)	-0,001 (0,006)	dust (dust/urban)
	BB	1,80 (1,81)	1,23 (1,08)	0,008 (0,01)	dust/BB (urban)
APO	WET	2,15 (2,04)	0,84 (0,82)	0,11 (0,10)	urban (urban)
	DRY	1,39 (1,38)	1,06 (1,10)	0,006 (-0,02)	dust (dust)
	BB	1,56 (1,61)	1,14 (1,20)	-0,008 (-0,01)	dust/BB (dust/BB)
NES	WET	2,05 (1,67)	0,72 (0,66)	0,13 (0,12)	urban (urban)
	DRY	1,74 (1,83)	1,06 (1,09)	-0,008 (0,003)	dust/urban (dust)
	BB	1,89 (1,80)	0,95 (1,07)	0,002 (0,02)	dust/urban (urban)

Table 2: Median aerosol Angström exponents of turbulent condition (stable condition) for each cluster and seasons measured at the CHC station and resulting aerosol types.

Aerosol type	SAE	AAE	SSAAE
Dust	-	> 0,9	[-0,05 ; 0,05]
Urban pollution	> 1,4	< 0,9	> 0,05
Biomass burning	-	> 1,1	[-0,05 ; 0,05]

Table 3: Updated Angström exponent values expected for aerosol types at the CHC station.

l.127: “As a summary, Table 1 shows expected Angström exponent for dust, urban pollution and Biomass Burning particules according the different referenced works (Dubovik et al., 2002 ; Collaud Coen et al., 2004 ; Clarke et al., 2007 ; Russel et al., 2010). This information has to be taken with caution since source influences are expected homogeneous and have been reported from several regions.”

l.482: “Table 2 summarizes the median Angström exponents measured at the CHC station for turbulent conditions (stable conditions in parenthesis). According to these values and as discussed above, aerosol types for the turbulent conditions (and stable conditions in parenthesis) are given.”

l.525: “A new Angsrtöm exponent classification can then be defined for measurement at the CHC station and is reported Table 3. Thresholds are close to the ones proposed by previous works (Dubovik et al., 2002 ; Collaud Coen et al., 2004 ; Clarke et al., 2007 ; Russel et al., 2010) but adapted to CHC’s instruments and particular atmospheric conditions.”

The source region analysis performed in this work is puzzling. I am not sure how source regions have been distinguished. As an example C6 and C4 seem to overlap on Fig 4b. The same holds for source regions C1 and C2. There is a second graph in the lower left corner of Fig 4b for which I could not find any explanation. What is this graph about and how it is different than the main one of Fig4b? Please improve the caption of Fig 4 to include all information so that the reader can decipher the plots easily. Some of the info required to do so are found in the text but definitely the info provided is not enough. Since you have performed this analysis for 4 years, the individual trajectories for each source region should be shown in a separate (for each source region) graph in the Appendix. Please also add another plot showing the average trajectories for each source region on a map. Hysplit has this ability to produce average trajectories and so other software that are free to use. Personally I would recommend that the average trajectories graph for each cluster to be included in Fig 4. However it is not mandatory.

Answer: Cluster definition is based on the statistical method described by Borge et al. (2007) now better described in the text. Hence, the six clusters correspond to the main directions of the BTs as shown by the map figure 4. C1 and C2 show clear difference between their main origins (less transparent cells in Figure 4a). About C4 and C6, the difference is much on the distance range from CHC station which can be seen on the zoom in on the lower left corner. C4 corresponds to shorter distance (within 100 km) and C6 corresponds to longer distance. Maps of the first 10% BTs of each cluster and selected for the study are added in the appendix and clearly helps to visualize these features.

Modifications:

Figure 4 has been improved according RC1 recommendations. Scales have been added and geographical references improved.

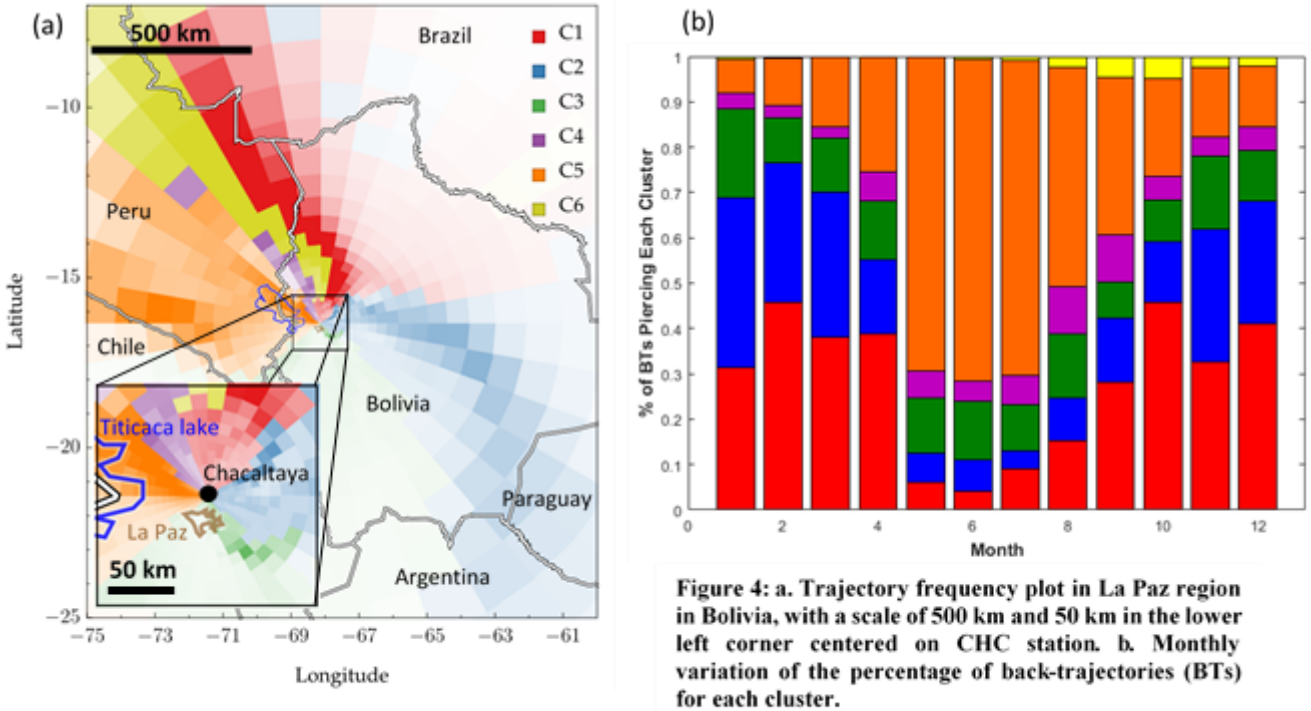

Figure 4: a. Trajectory frequency plot in La Paz region in Bolivia, with a scale of 500 km and 50 km in the lower left corner centered on CHC station. b. Monthly variation of the percentage of back-trajectories (BTs) for each cluster.

Appendix A1:

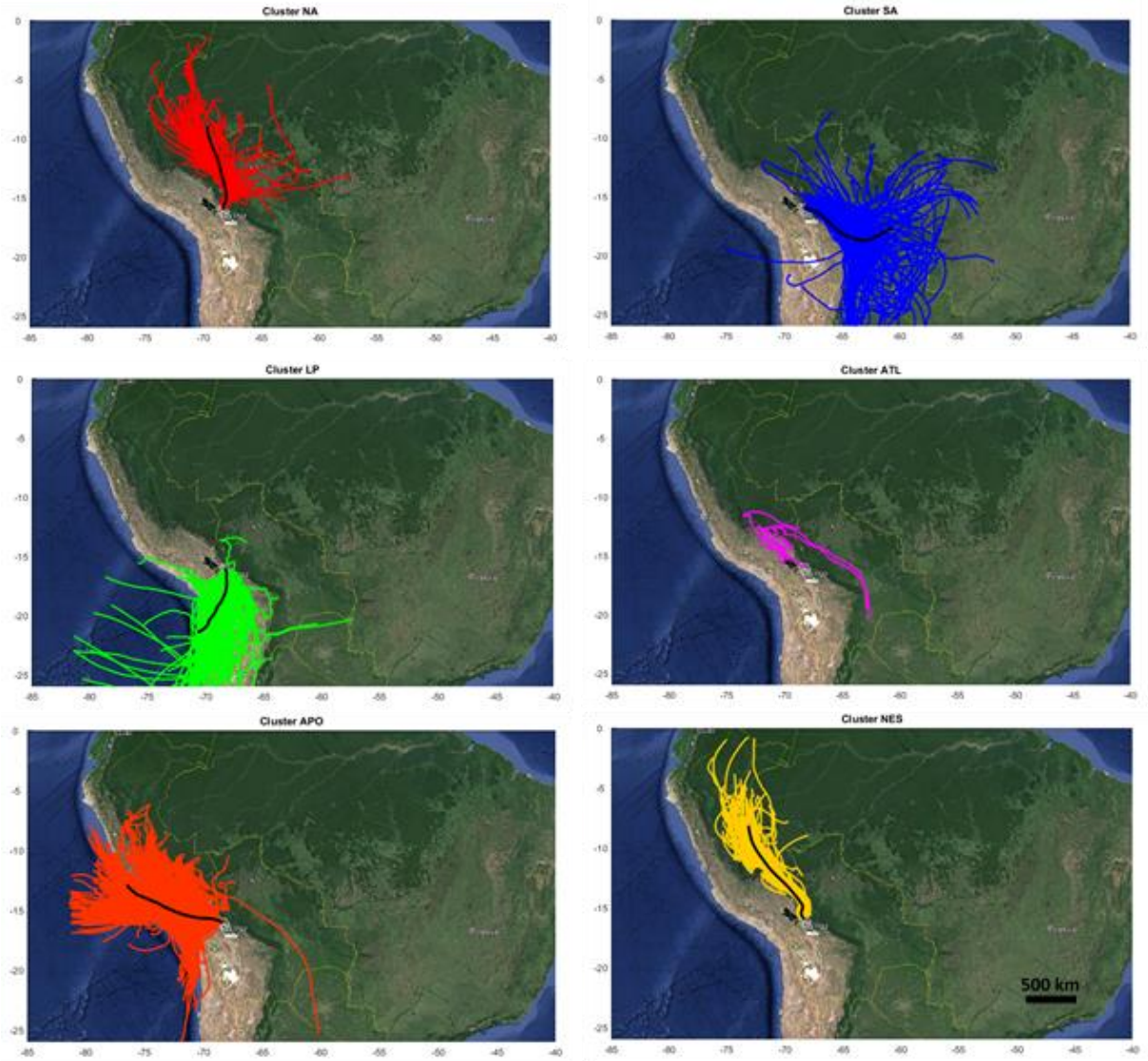

Figure A1: Selected 96-hours back-trajectories for the six clusters obtained from the Borge et al. (2007) method. The black line corresponds to the main back-trajectory.

l.554: "For each hour of the period of the study, nine back-trajectories have been used to describe the mean influence at Chacaltaya station. The nine BTs start within a square of 2 km by 2 km around the station. The mean BT has been calculated from these nine BTs and generated every hour from January 2012 to December 2015. Clusters are defined according the Borge et al. (2017) method using a two-stage technique (based on the non-hierarchical K-means algorithm). The Borge et al. (2007) method allows to attribute to each mean BT a fraction of each cluster according to their time residence into the cluster and their distance from the CHC station. Hence, BTs are sorted according to their representativeness in each cluster. The first 10% of them are used in the present study and are reported in Fig. (A1)."

l.301: "Finally, cluster 6 (NES) has properties close to cluster 1 but with less influence from the Amazonian Basin and close to cluster 4 but with aerosol sources further from CHC station (> 100 km)."

There is a problem with the term ε in Eq 11. Is sa and ca are the sine and cosine of the same angle then by definition ε=0 regardless. This is due to the well known formula of $\cos 2\theta+\sin 2\theta=1$. I suspect a typo.

Answer: s_a and c_a are the average value of sinθ and cosθ in the 15 minutes time interval. As described in Yamartino et al. (1984), $s_a \neq \sin\theta_a$, $c_a \neq \cos\theta_a$ and $s_a^2 + c_a^2 \leq 1$.

Modifications:

l.231: Definition of ε has been corrected : " $\varepsilon = \sqrt{1 - (s_a^2 + c_a^2)}$ "

l.232: definition of sa and ca have also been corrected : "with the averages $s_a = \frac{1}{N}\sum_{i=1}^{N} sin\theta_i$ and $s_a = \frac{1}{N}\sum_{i=1}^{N} cos\theta_i$ of N the number of horitontal wind direction (θi) recorded in 15 minutes."

In addition if σθ corresponds to the 15 minute average wind direction as stated in Line 179 what is the θ(15), θ(30), θ(45), θ(60) of Eq. 10. I thought they denoted different time intervals. Please spend some effort to explain further how the classification shown in Fig.2 is performed. In other words explain further what is discussed in Lines 181 and 182.

Answer: $\sigma^2_{\theta(15)}$ corresponds to the squared standard deviation of the horizontal wind direction calculated every 15 minutes. These quantities are later hourly averaged.

Indeed, atmospheric layer definitions are largely discussed on aerosol and dynamic studies, and according to the method used, the definitions of the layers are slightly different. In the present study, because we use atmospheric stability as tracer for atmospheric layers, it is more appropriate to use the two different regime "stable conditions" and "turbulent conditions".

Modifications:

In the full document, "layer" has been replaced by "condition" when needed, and SL – TL has been replaced by SC – TC (Stable and Turbulent Conditions).

l.220: "In addition, a residual layer can also be present at CHC station during nightime, resulting from low dispersion of the daytime convection. Because no clear distinctions between the mixing, the free tropospheric, and the residual layers can be strictly obtained from in-situ measurements only, the present dataset recorded at Chacaltaya station is separated in terms of stability conditions (turbulent and stable)."

l.227: "This method is based on the hourly averaged value of the standard deviation of the horizontal wind direction (σ_θ in Eq. 10) calculated every 15 minutes"

l.229: "with $\sigma_{\theta(15)}$ the standard deviation of the horizontal wind direction calculated on the first 15 minutes of every hour, and $\sigma_{\theta(60)}$ the last 15 minutes of every hour."

l.237: "As described in Rose et al. (2017), the classification depends also on the σ_θ value in the 4-hour time interval across the time of interest. Interface cases correspond to unclassified data which mainly show a high variability of the standard deviation between the two categories of dynamic. For clarity, the interface cases are excluded from the dataset in the rest of the paper."

Despite that most of this work relates to phenomenology, there are two important findings. These are the very low AAE reported during the wet season and the linear relationship between SSAAE and AAE observed during the wet and dry seasons. I am wondering if such low AAE have been reported elsewhere in literature. Please discuss. Can the authors provide an explanation on the linear relationship observed in Fig9a?

Answer: The present study shows AAE reaching 0.5. These values are also observed by Russel et al. (2010) and corresponds to "urban industrial" impacts. AAE values from 1,5 to 3 correspond to dust particles.

The linear relationship between SSAAE and AAE can mainly be explained by a similarity on the sensibility to the two properties to two aerosol type. When air masses are mainly influenced by urban particles, especially during the wet season for every clusters, AAE values are close to 1 (or lower than BB influences) and SSAAE values are higher than 0. In the other hand, when air masses are mainly influenced by dust and BB particles (dry season for every clusters), AAE values are close to 2 (or much higher than during urban influences) and SSAAE values are close or below 0. A mixture between these two aerosol types will lead to intermediate values located in line with them.

Modifications:

l.445: "As shown in Fig. 5, low AAE values, especially during the wet season, can be explained by important reduction of dust and less biomass burning particles due to more efficient removal."

l.450: "Thus, the wet season presents positive SSAAE and AAE close or lower than 0.9, while dry season and BB period present SSAAE close to 0 and AAE higher than 0.9. A linear relationship between AAE and SSAAE values is observed and illustrates that mainly urban emissions drive aerosol particle properties during the wet period, and that mainly dust emissions drive aerosol particle properties during the dry season and the BB period."

There is a typo in the caption of Appendix Fig A1. Aerosol should probably be absorption and for the entire dataset instead of the all dataset

Answer: True

Modifications:

"Figure A2: Weekly variation of the Absorption Angström Exponent (AAE) for the whole dataset from 2012 to 2015. The medians and their 25th and 75th percentiles from Sundays to Saturdays are represented. "

Interactive comment on Atmos. Chem. Phys. Discuss., https://doi.org/10.5194/acp-2019-510, 2019.

References:

Borge, R., Lumbreras, J., Vardoulakis, S., Kassomenos, P. and Rodríguez, E.: Analysis of long-range transport influences on urban PM 10 using two-stage atmospheric trajectory clusters, Atmos. Environ., 41(21), 4434–4450, 2007.

Clarke, A., McNaughton, C., Kapustin, V., Shinozuka, Y., Howell, S., Dibb, J., Zhou, J., Anderson, B., Brekhovskikh, V., Turner, H. and Pinkerton, M.: Biomass burning and pollution aerosol over North America: Organic components and their influence on spectral optical properties and humidification response, J. Geophys. Res. Atmospheres, 112(D12), D12S18, doi:10.1029/2006JD007777, 2007.

Collaud Coen, M., Weingartner, E., Apituley, A., Ceburnis, D., Fierz-Schmidhauser, R., Flentje, H., Henzing, J. S., Jennings, S. G., Moerman, M., Petzold, A., Schmid, O. and Baltensperger, U.: Minimizing light absorption measurement artifacts of the Aethalometer: evaluation of five correction algorithms, Atmospheric Measurement Techniques, 3(2), 457–474, doi:10.5194/amt-3-457-2010, 2010.

Dubovik, O., Holben, B., Eck, T. F., Smirnov, A., Kaufman, Y. J., King, M. D., Tanre, D. and Slutsker, I.: Variability of absorption and optical properties of key aerosol types observed in worldwide locations, J. Atmospheric Sci., 59, 590–608, doi:Review, 2002.

Rose, C., Sellegri, K., Moreno, I., Velarde, F., Ramonet, M., Weinhold, K., Krejci, R., Andrade, M., Wiedensohler, A. and Ginot, P.: CCN production by new particle formation in the free troposphere, Atmospheric Chemistry and Physics, 17(2), 1529–1541, 2017.

Russell, P. B., Bergstrom, R. W., Shinozuka, Y., Clarke, A. D., DeCarlo, P. F., Jimenez, J. L., Livingston, J. M., Redemann, J., Dubovik, O. and Strawa, A.: Absorption Angstrom Exponent in AERONET and related data as an indicator of aerosol composition, Atmospheric Chem. Phys., 10, 1155–1169, doi:10.5194/acp-10-1155-2010, 2010.

Yamartino, R. J.: A comparison of several “single-pass” estimators of the standard deviation of wind direction, J. Clim. Appl. Meteorol., 23(9), 1362–1366, 1984.

Anonymous Referee #4

Received and published: 3 September 201

First, authors would like to thank the reviewer for his/her constructive and detailed suggestions. Their additions to the paper helping us to improve significantly the clarity and the precision of the method used and the robustness of the results.

The atmospheric stability is used as a tracer to differentiate the atmospheric layers. As recommended, Stable Layer (SC) and Turbulent Layer (TL) are have been replaced by Stable Conditions (SC) and Turbulent Conditions (TC). This was also requested by other 2 reviewers.

In the following, we provide answers to the reviewer's comments and list modifications made in the manuscript.

This paper provides an interesting overview of the aerosol particle properties observed at the high mountain station Chacaltaya in the South America (Cordillera Real). The topic is of interest for ACP and the paper is generally well written. The scientific approach is sufficiently robust and the presentation of data and results is fair. Nevertheless, some points should be better addressed before publications. In particular, the authors should better discuss the caveats related with the back-trajectories analysis as well as provide more details and information about the experimental methodologies (e.g., no information about data generation, uncertainty characterization are provided).

In the following you can find my specific comments. ——————————————— ——————— ———————————————

Abstract. In the last sentence, the authors claimed that "CHC provides first evidences of impact of emission from Amazonian basin far away from their source". Be more specific. Which "far away" means? Please, in the site description provide distance of CHC from Amazonian basin.

Answer: The CHC station is described as a background GAW site and is located 17 km from the first urban area, and around 300 km from fire area in Bolivia (Carmona-Moreno et al. 2005, Giglio et. al 2013). The Rondonia region where a significate deforestation process is reported every year is located 800 km from CHC station. In addition, CHC is the highest GAW station in the world and unique free tropospheric conditions can be obtained in the region where particles and gases have residence time of several months and be transported over large distances.

Modifications:

l.56: "From this analysis, long-term observations at CHC provides the first direct evidence of the impact of Biomass Burning emissions of the Amazonian basin and urban emissions from La Paz area on atmospheric optical properties to a remote site all the way to the free troposphere."

l.148: "[...] (Carmona-Moreno et al. 2005, Giglio et. al 2013). Indeed, the closest region where large areas are affected by biomass burning activities is the Bolivian Amazonia (Beni, Santa Cruz, north of La Paz departments) located ca. 300 km from the station, north and eastward from the Andes mountain range."

Line 71: please provide wavelengths.

Answer: Husar et al., (2000) reports aerosol extinction coefficients values related to visibility. Their values are representative of the integrated visible range. In this condition, it may not be reliable to

compare those aerosol extinction coefficients with the Chacaltaya measurements. However, the study gives an interesting analysis of the impact of Amazonian fires at different altitudes and different distances to the main fire activities.

Modifications:

l.84: “Between the wet season and the biomass burning season, Schafer et al. (2008) show an increase of Aerosol Optical Depth by a factor of 10 from AERONET sites in southern forest region and the Cerrado region and, by a factor of 4 in the northern forest region.”

l.88: “The study reports a spatial pattern of the visibility between 100 and 200 Mm-1 over the Amazon Basin. However, values can reach 600 Mm-1 at Sucre station (2903 m above sea level, hereafter abbreviated as “a.s.l.”), 1000 Mm-1 at Vallegrande (1998m a.s.l.) and 2000 Mm-1 at Camiri (792 m a.s.l.) during BB period. Even the study clearly shows impacts of Amazonian activities at different altitudes and long distances, only few studies report long time period of aerosol optical properties.”

l.96: “These extremely high coefficients are due to the proximity to BB sources for FNSA station and its very low altitude.”

Line 92 – 105: this section ìs hard to follow. I would recommend to add a table with the different threshold values for each type of particles (dust, pollution, biomass burning) for the different Angstrom exponents (AAE, SAE, SSAE).

Answer: Three tables have been added to the text which summarize information from the text. The Table 1 summarizes ranges of Angström exponent for the different aerosol types. Table 2 details the median values of the Angström exponent for each cluster, season and atmospheric stability. Table 3, on the conclusion, suggests a new Angtsröm exponent definition for the different aerosol types.

Modifications:

Aerosol type	SAE	AAE	SSAAE
Dust	Close to 1	Close to 1	Below 0
Urban pollution	Close to 2	Close to 1	Higher than 0
Biomass burning		Close to 2,1	

Table 1: Expected aerosol type and their optical properties for each cluster according season and atmospheric stability.

Cluster	season	SAE	AAE	SSAAE	Aerosol types
NA	WET	2,04 (1,42)	0,58 (0,56)	0,18 (0,15)	urban (dust/urban)
	DRY	1,91 (1,80)	1,00 (1,01)	0,01 (0,004)	urban (dust)
	BB	1,92 (1,87)	1,10 (1,26)	0,03 (0,02)	dust/BB (dust/BB)
SA	WET	1,2 (1,40)	0,74 (0,68)	0,11 (0,11)	urban (urban)
	DRY	1,69 (1,70)	1,04 (0,96)	0,02 (0,03)	dust (dust)
	BB	2,16 (2,02)	1,23 (1,20)	0,005 (0,01)	BB (BB)
LP	WET	1,71 (2,09)	0,86 (0,82)	0,08 (0,10)	urban (urban)
	DRY	1,64 (1,74)	1,05 (1,07)	0,02 (-0,01)	urban (dust/urban)
	BB	1,49 (1,93)	1,09 (1,29)	-0,02 (-0,02)	dust (dust/BB)
ATL	WET	1,93 (2,11)	0,75 (0,65)	0,11 (0,15)	urban (urban)
	DRY	1,77 (1,94)	1,00 (1,05)	-0,001 (0,006)	dust (dust/urban)
	BB	1,80 (1,81)	1,23 (1,08)	0,008 (0,01)	dust/BB (urban)
APO	WET	2,15 (2,04)	0,84 (0,82)	0,11 (0,10)	urban (urban)
	DRY	1,39 (1,38)	1,06 (1,10)	0,006 (-0,02)	dust (dust)
	BB	1,56 (1,61)	1,14 (1,20)	-0,008 (-0,01)	dust/BB (dust/BB)
NES	WET	2,05 (1,67)	0,72 (0,66)	0,13 (0,12)	urban (urban)
	DRY	1,74 (1,83)	1,06 (1,09)	-0,008 (0,003)	dust/urban (dust)
	BB	1,89 (1,80)	0,95 (1,07)	0,002 (0,02)	dust/urban (urban)

Table 2: Median aerosol Angström exponents of turbulent condition (stable condition) for each cluster and seasons measured at the CHC station and resulting aerosol types.

Aerosol type	SAE	AAE	SSAAE
Dust	-	> 0,9	[-0,05 ; 0,05]
Urban pollution	> 1,4	< 0,9	> 0,05
Biomass burning	-	> 1,1	[-0,05 ; 0,05]

Table 3: Updated Angström exponent values expected for aerosol types at the CHC station.

l.127: “As a summary, Table 1 shows expected Angström exponent for dust, urban pollution and Biomass Burning particles according the different referenced works (Dubovik et al., 2002 ; Collaud Coen et al., 2004 ; Clarke et al., 2007 ; Russel et al., 2010). This information has to be taken with caution since source influences are expected homogeneous and have been reported from several regions.”

l.482: “Table 2 summarizes the median Angström exponents measured at the CHC station for turbulent conditions (stable conditions in parenthesis). According to these values and as discussed above, aerosol types for the turbulent conditions (and stable conditions in parenthesis) are given.”

l.525: “A new Angtsröm exponent classification can then be defined for measurement at the CHC station and is reported Table 3. Thresholds are close to the ones proposed by previous works (Dubovik et al., 2002 ; Collaud Coen et al., 2004 ; Clarke et al., 2007 ; Russel et al., 2010) but adapted to CHC’s instruments and particular atmospheric conditions.”

Line 103: please correct "bellow"

Modifications: “bellow” has been corrected by “below”

Line 135: please clearly state which kind of compensation must be applied to aethalometer data.

Answer: Weingartner et al. (2003) correction is applied in order to compensate the multi-scattering effects and the loading effects on the aethalometer’s filters. The correction is performed by adjusting the f factor showed in equation 3.

Modifications:

l.170:“Aethalometer measurements were compensated for multi-scattering effects and loading effects (or shadowing effects) following the method described by Weingartner et al. (2003) briefly explained below.”

Line 140. was the mass coefficient provided by the manufacturer independently assessed and validated by others? If yes, provide references, if not, provide adequate comments

Answer: The mass coefficient given by the manufacturer allows us to convert BC concentrations to attenuation coefficients as derived from the Mie theory for small uniform spheres. Hence, the mass coefficient is inversely proportional to the optical wavelength as follow: σ= 14625 / λ, which corresponds to sigma values between 15 and 40 m^2 g^{-1} for wavelengths between 370 and 950 nm. Liousse et al. (1993) demonstrated highly variable mass coefficients depending on aerosol type and age. Saturno et al. (2017) recently demonstrate agreement between aethalometer corrections using manufacturer’s sigma coefficients and other instruments as MAAP and a multiple-wavelength absorbance analyser (MWAA). Collaud Coen et al. (2010) also demonstrate Weingartner’s correction as a good compromise comparing to Schmid’s et al. (2006) correction and Arnott’s et al. (2005) correction.

Modifications:

l.176: “with σm the mass coefficients given by the instrument’s instructions (The Aethalometer, A.D.A. Hansen, Magee Scientific Company, Berkley, California, USA) and based on the Mie theory. σm strongly depends on the aerosol type and age (from 5 to 20 m² g-1, Liousse et al., 1993). However, the manufacturer values (14625 nm m2 g-1 λ-1) have been recently validated in a comparison study between ifferent aethalometer corrections (Collaud Coen et al. 2010 ; Saturno et al., 2017).”

The method for deriving the absorption coefficient it is not clear. Equation 2, what is C.R(ïA¸˘n)?. Equation 3 it is also not clear: please describe the contribution of each member/factor. What ln(10%) and ln(50%) represent? Why the factor R should be adjusted? What do you mean for "spot" change? Why the absorption coefficient should be the same before and after the spot change?

Answer: “C.R(ïA¸˘n)” is probably due to format issues and should be C.R(λ). Then, C is defined as the calibration factor constant with wavelength, and R another calibration factor which does depend on the wavelength.

The aethalometer instrument permits to obtain aerosol absorption coefficients from optical measurement of aerosol trapped on a filter. Every 5 minutes, the spot on the filter band is changed in order to reduce loading effects. Hence, absorption coefficients from one spot to the other should not

change significantly, then the median ratio between two successive absorption retrievals should be less than 1.

The method to derive absorption coefficients and correct data from aethalometer issues (multi-scattering and loading effect) is briefly described in this paper. However, the method is described in details in Weingartner et al. (2003) and largely used in other several studies (Bond et al., 2006, 2013 ; Rose et al., 2015 ; Andreae and Gelencsér, 2006 ; Zotter et al., 2017 ; Rajesh and Ramachandran, 2018). If C allows to correct multi-scattering effects linked to filter properties, R has to be adjusted in order to correct the loading effect and is related to wavelength and aerosol properties trapped on the filter. In Weingartner et al. (2003), we can find the description of every member. f is the filter loading effect compensation parameter and represents the slope of the curve of R as function of $\ln(\sigma_{atn})$ for a σ_{atn} change from 10% to 50%.

Modifications:

l.167: “Every 5 minutes, the spot on the filter band is changed in order to reduce loading effects.”

l.170: “Aethalometer measurements were compensated for multi-scattering effects and loading effects (or shadowing effects) with the method described by Weingartner et al. (2003) and briefly explained below.”

l.176: “with σ_m the mass coefficients given by the instrument’s instructions (The Aethalometer, A.D.A. Hansen, Magee Scientific Company, Berkley, California, USA) and based on the Mie theory. σ_m strongly depends on the aerosol type and age (from 5 to 20 m^2 g-1, Liousse et al., 1993). However, the manufacturer values (14625 nm m2 g-1 λ-1) have been recently validated in a comparison study between aethalometer corrections (Collaud Coen et al., 2010 ; Saturno et al., 2017).”

l.182: “with C = 3.5 a calibration factor linked to multiple-scattering and assumed constant according wavelengths (GAW Report No. 227), and R, a calibration factor which depends on aerosol loading on the filter and aerosol optical properties, calculated as: [...]”

l.186: “where f is the filter loading effect compensation parameter and represents the slope of the curve of R as function of $\ln(\sigma_{atn})$ for a σ_{atn} change from 10% to 50%”

Equation 4: what "mEBC" is? Does QEBC is equal to QBC reported by line 148?

Answer: EBC corresponds to Equivalent Black Carbon. Because Black Carbon concentrations are obtained from optical measurements, and assumptions on mass absorption cross-section coefficients have to be included, it seems more appropriate to use Equivalent Black Carbon. Q_{BC} should be Q_{EBC} everywhere in the manuscript.

Modifications:

l.191: “A mass absorption cross-section Q_{EBC} = 6.6 $m^2.g^{-1}$ at 670 nm is used to determine Equivalent Black Carbon mass concentrations”

Line 155: the authors stated that the aethalometer measurement at 635 mm is unstable. Quantitatively, what does this mean? Do you are able to provide threshold value that other users can apply to evaluate if their own measurements are unstable? In general, which QA/QC framework/procedures did you apply to all the suite of measurement discussed in this work? Please

describe air inlet system and calibration strategies for the considered instrumentations (i.e. nephelometer, aethalometr, MAAP). Please quantify uncertainties related to each of these measurements.

Answer:

Indeed, nephelometer measurements at 635 nm do show unstable values during several days. The figure below shows an example of these unstable periods, here for the scattering coefficients at 450, 525 and 635 nm between the 7th of September to the 9th of September 2012. The wavelength dependence of the scattering coefficients suddenly changes the 7th of September around 6 pm and the 635 nm channel keeps high values for several months. Level 2 data used in this work are in the EBAS database and consequently these data are controlled and opportunely flagged when issues were observed. The authors decided to only use unchanged 450 and 525 nm channels to analyse aerosol optical properties at Chacalataya.

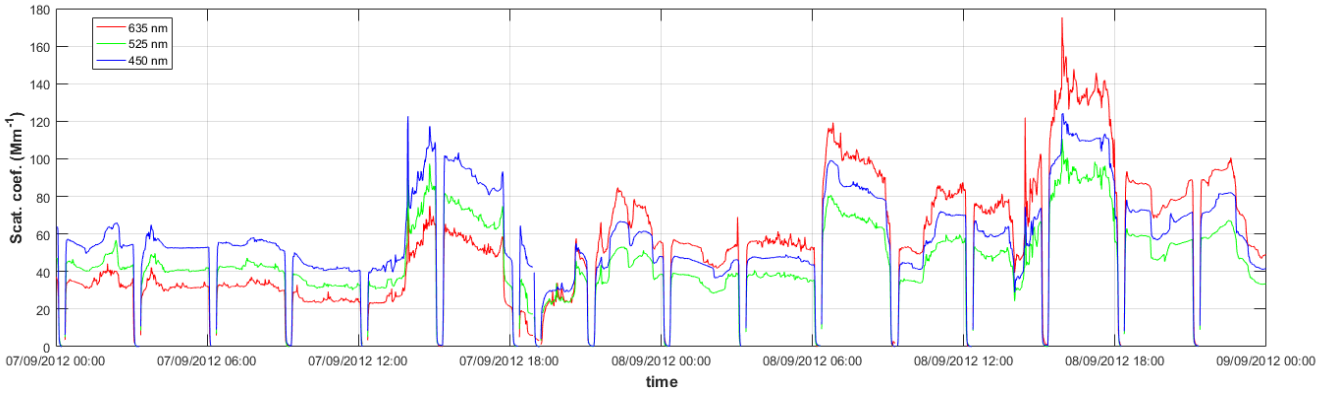

Figure 1: Temporal serie of the scattering coefficients at 450, 525 and 635 nm retrieved from the nephelometer at Chacaltaya station between the 7th of September at 00 am to 9th of September 2012 at 00 am.

From optical property measurements, the full dataset between the 3rd of January 2012 to 30th of November 2015 has been used. Every in-situ instruments of the station are located downstream a Whole Air Inlet and a dryer.

The nephelometer instrument was periodically calibrated using CO_2 as span gas and frequent zero adjusts were performed, following the procedure described in Ecotech manual (2009). The uncertainty of the Aurora 3000 is given in the user manual to be 2,5 %.

The air-flow and the absorption cross-section of the aethalometer instrument are calibrated. The method is detailed on the Magee Scientific manual (REF). Accuracy of attenuation coefficients are around 5%.

The MAAP instrument is automatically calibrated for air-flow, temperature and pressure according to the instruction manual (Model 5012 Instruction Manual) and described in Petzold and Schönlinner, 2004). According to them, uncertainty of the absorbance is 12%.

Modifications:

l.156: “In-situ instruments of the station operated behind a Whole Air Inlet equipped with an automatic dryer (activated above 90% RH) .”

l.158: “In the current study, the full dataset of in-situ optical measurements has been used between January 2012 and December 2015.”

l.169: “Sensor calibration is performed automatically and an uncertainty of 5 % on attenuation coefficients is given by the constructor.”

l.190: “According to Petzold and Schönlinner (2004), uncertainty of the absorbance is 12%.”

l.198: “The nephelometer instrument is calibrated using CO_2 as span gas and frequent zero adjusts were performed, following the procedure described in Ecotech manual (2009). The uncertainty of the Aurora 3000 is given in the user manual to be 2,5 %.”

Also equation 10 is not clear: what σÏt’2 (x) with X=12,30,45,60 represent? I think that the vocabulary used by the authors can be misleading. More than layers this methodology can be able to discriminate turbulent versus stable (or more stable) conditions at the measurement site. Please change nomenclature.

Answer: $\sigma^2_{\theta(15)}$ corresponds to the squared standard deviation of the horizontal wind direction calculated every 15 minutes. Hence, the standard deviation of the horizontal wind direction is calculated every 15 minutes and then hourly averaged.

Indeed, atmospheric layer definitions are largely discussed on aerosol and dynamic studies, and according to the method used, the definitions of the layers are slightly different. In addition, a residual layer can also be present at CHC station during nighttime, resulting from low dispersion of the daytime convection. In the present study, because we use atmospheric stability as tracer for atmospheric layers, it is more appropriate to use the two different regime “stable conditions” and “turbulent conditions”.

Modifications:

In the full document, “layer” has been replaced by “condition” when needed, and SL – TL has been replaced by SC – TC (Stable and Turbulent Conditions).

l.220: “In addition, a residual layer can also be present at CHC station during nighttime, resulting from low dispersion of the daytime convection. Because no clear distinctions between the mixing, the free tropospheric, and the residual layers can be strictly obtained from in-situ measurements only, the present dataset recorded at Chacaltaya station is separated in terms of stability conditions (turbulent and stable).”

l.227: “This method is based on the hourly averaged value of the standard deviation of the horizontal wind direction (σ_θ in Eq. 10) calculated every 15 minutes”

l.229: “with $\sigma_{\theta(15)}$ the standard deviation of the horizontal wind direction calculated on the first 15 minutes of every hour, and $\sigma_{\theta(60)}$ the last 15 minutes of every hour.”

Line 189: why was the residual layer excluded by the analysis? Does this mean that the residual layer conditions are embedded in what the author defined as "stable" layers? Please, better specify this point since this can have implications for the interpretation of results.

Answer: The residual layer is finally reported as stable condition. Hence, the interface cases do not take into account the residual layer but cases which cannot be attributed to stable or turbulent conditions. Indeed, these cases correspond to unclear dynamical conditions with high variability of the

standard deviation of the horizontal wind direction. In order to analyse aerosol properties in stable and turbulent conditions only, the interface measurements have to be excluded.

Modifications:

I.220: “In addition, a residual layer can also be present at CHC station during nightime, resulting from low dispersion of the daytime convection. Because no clear distinctions between the mixing, the free tropospheric, and the residual layers can be strictly obtained from in-situ measurements only, the present dataset recorded at Chacaltaya station is separated in terms of stability conditions (turbulent and stable).”

l.236: “Interface cases correspond to unclassified data which mainly show high variability of the standard deviation between the two categories of dynamic. As described in Rose et al. (2017), the classification depends also on the σ_θ value in the 4-hour time interval across the time of interest. Interface cases correspond to unclassified data which mainly show a high variability of the standard deviation between the two categories of dynamic. For clarity, the interface cases are excluded from the dataset in the rest of the paper.”

l.249: “Black spots represent undefined cases (or interface) due to a fluctuating classification within the 1-hour time window.”

l.500: “Even TC is usually attributed to mixing layer, SC can be undoubtedly attributed to free tropospheric or residual layers.”

Line 193: I think that "morning" must be changed by "night"

Answer: True.

Modifications:

l.250: “This 3-day example shows that SLSC conditions are mostly observed during night when the convective effect of the previous day is already dissipated and no convective effect of the current day is present.”

Line 204: what BT set is used for the cluster analysis (12 hours or 96 hours)? Why different TRJ lengths were considered/calculated? Is the trajectory calculation set-up changing for the 12 and the 96 hours BTs? The authors did not provide any indication about the meteorological files (which are? Which horizontal and vertical resolution?) used for BT calculation nor about calculation set-up (which starting heights? single or multiple starting points around the station locations). The resolution of the input metro files is particularly important in this mountain region, I guess. Please comment on that and provide caveats about the effective reliability of trajectories in this region. This point is critical for interpretation of results.

Answer:

Indeed, only 96 hours back-trajectories are used in cluster analysis. 96-hours BTs are more appropriate in this region to analyse long range transports in particular from the Amazonian forest.

Hysplit trajectories has been generated using WRFd04 data and the kinematic method with ERA-interim data as boundary conditions. This dataset presents the best topographic resolution for this region with spatial resolution of 1.06x1.06 km and give an altitude of Chacaltaya station of 5058 m

a.s.l. (true altitude 5240 m a.s.l.). The WRF dataset presents 28 atmospheric levels of pressure given every 6 hours. For this study, 96-hours BTs are generated every hour starting at 9 locations around the Chacaltaya station (Table 4 below).

Latitude (degrees)	Longitude (degrees)	Altitude (m a.s.l.)
-16,36	-68,14	4852
-16,35	-68,14	4918
-16,34	-68,14	4883
-16,36	-68,13	5000
-16,35	**-68,13**	**5058**
-16,34	-68,13	4965
-16,36	-68,12	5042
-16,35	-68,12	5043
-16,34	-68,12	4936

Table 4: Positions of the 9 stating location of BTs calculations. Chacaltaya station is bolded.

Modifications:

l.264: “WRFd04 dataset has been used to generate BTs every hour, starting at nine locations at less than 1 km around the Chacaltaya station (within a square of 2x2 km around the station). This dataset presents the best topographic resolution for this region with spatial resolution of 1.06x1.06 km, and 28 pressure levels.”

Figure 4a is hard to understand and the comparison among the different cluster is challenging. Maybe, it can help to use a stack bar plot with 1 bar for each single month composed by the contribution from each different single cluster.

Also Figure 4b is difficult. The geographical boundaries are not clear at all. The same is true for the topographic features. Most of the locations listed in the legend are meaningfulness for readers not used with the region (are these villages, cities, regions?). For these reasons, it should be strongly improved.

Answer: Figures 4a and 4b have been improved. Indeed, stack bars allow to compare contribution of each cluster every month and is better appropriate to details given in the text. As recommended by RC1, trajectories of each cluster have also been added to Appendix A to illustrate results of the cluster analysis method.

Modifications:

Figure 4a and 1b have been improved.

legend Figure 4: “a. Trajectory frequency plot in La Paz region in Bolivia, centered on Chacaltaya station. ba. Monthly variation of the percentage of back-trajectories (BTs) for each cluster.”

Appendix A added with the 10% first BTs more representative of each cluster.

Line 212: sentence starting with "Thus, for each cluster,..." isnt.t clear: what do you mean for "events"? " When the cluster have the most influence”: what does it mean?

Answer: In order to obtain aerosol optical properties of each cluster, only a part of the back-trajectories have been selected. One BT is selected if its contribution to one cluster is high enough.

Hence, this can be obtained by selecting the first 10% of the BTs which are the most representative of each cluster. The describing paragraph has been improved to explain this selection of BTs.

Modifications:

l.268: "The Cluster Analysis method used in this study is described in Borge et al. (2007) and based on the Euclidean geographical coordinates distance and given time intervals. Figure (4a) shows the trajectory frequency plot. The opacity of each pixel is proportional to the number of BTs passing through each grid cell. Clusters are defined by using a two-stage technique (based on the non-hierarchical K-means algorithm). Six clusters have been found around the Chacaltaya station. Hence, a fraction of each cluster is assigned to each BT, and is calculated according the residence time in each cluster and their distance from the reference location (the Chacaltaya station). In order to obtain aerosol optical properties of each cluster, only a part of the back-trajectories have been selected. One BT is selected if its contribution to one cluster is high enough. For each cluster, the first 10% of the BTs have been selected by demonstrating the highest contribution to one any cluster. This firsts 10% of BTs related to each clusters and their mean paths are shown in Appendix A1

Line 263: Since the extinction is the sum of absorption and scattering, and scattering » absorption, the similarity between extinction and scattering is trivial.

Answer: This sentence permits to show that the extinction coefficient is mainly driven by the scattering property. This is regularly the case and can be deleted here.

Modifications:

l.333: "[...] and follows a seasonal variation that is very similar to the one of the scattering coefficient" has been deleted.

Line 377 - 376: please better explain. in which way the AAE values are impacted by the aethalometer variability. Do you mean that the uncertainty of aethalometer is enhanced during wet season? For which reason? How this impact results robustness (please discuss in the conclusions)?

Answer: The absorption Angtström exponent is calculated according equation 7 by using wavelength dependency of the absorption coefficients measured by the Aethalometer. As described in the description of the Aethalometer correction, absorption measurements can be biased by an important aerosol loading on filters and multi-scattering effects. However, two physical ways can explain these low AAE values: a reduction of dust and less biomass burning particles due to more efficient removal (higher hygroscopicity of BB particles). The Figure shows the frequency plot of the AAE for the entire period. Results are centered around 1 but vary from -0.5 to 2.

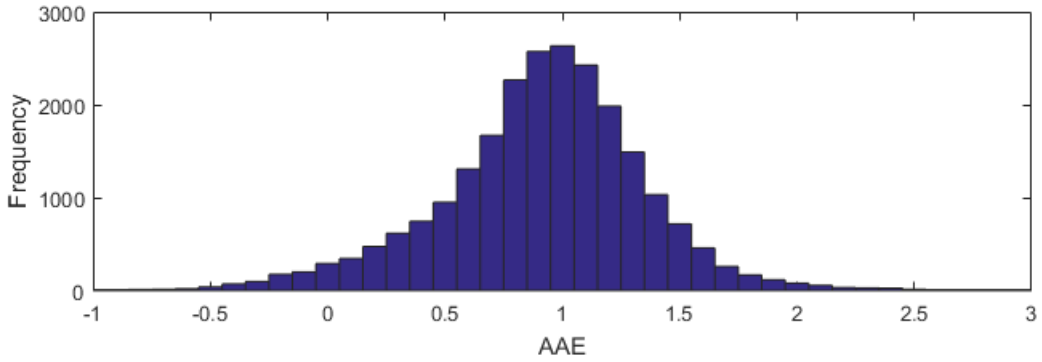

Figure 2 : Frequency plot of the Absorption Angström Exponent for the full period of the study.

Modifications:

l.445: "As shown in Fig. 5, low AAE values, especially during the wet season, can be explained by important reduction of dust and less biomass burning particles due to more efficient removal."

Line 401: the decrease of urban particle influence within air-masses from LaPaz during "turbulent" conditions (in which I expect more efficient transport from the lower layers to CHC) is rather surprising. Does this indicate some inaccuracies in the local TRJ calculation or in the turbulent conditions identification?

Answer: Capturing the local atmospheric stability is still highly challenging in this region due to the complex topography and high altitude. In addition to these inaccuracies, and as mentioned in the text, dust particles largely generated in this region can also affect measurements in turbulent conditions measured at Chacaltaya station and thus, decrease SAE values. It can also be noticed that SSAAE are still representative of urban influences with values above 0. This indicates the main influence of urban particles from LP cluster in both stability conditions but with a moderate addition of dust influence in the turbulent condition cases.

Modifications:

l.474: "In addition to urban influences, during the BB period and the wet season, LP air masses are also affected by dust particles, especially in the TC, with significantly lower SAE values in the TL."

Line 421:I agree that the transport to higher troposphere layers was supported but the spread over long-range (please, quantitatively specify what do you mean for longrange) is more a (reliable) hypothesis.

Answer: The long-range transport from the aerosol sources still a challenge to define since no detailed analysis is available about aerosol source locations. However, for BB emissions, the first intensive biomass burning source is located at 300 km fare from Chacaltaya station.

Modifications:

l.148: "[...] (Carmona-Moreno et al. 2005, Giglio et. al 2013). Indeed, the closest region where large areas are affected by biomass burning activities is the Bolivian Amazonia (Beni, Santa Cruz, north of La Paz departments) located ca. 300 km from the station, north and eastward from the Andes mountain range."

l.505: “The present study has hence demonstrated that BB particles are efficiently transported to the higher part of the troposphere (Stable conditions) and over long distances (more than 300 km long).”

Line 435: the authors concluded that an effect of dust is visible during the entre dry season. However, looking at figure 9, SSAAE is mostly >0 during the dry season which contradict this (see also line 103). Please comment and/or rephrase.

Answer: In this arid region, dust sources have a significant impact on ground based measurements especially when the station is in turbulent conditions which tend SSAAE values to be below 0. However, air masses are not purely influenced by dust particles and are always slightly impacted by urban or BB emissions. In these conditions, SSAAE values are close to 0. In addition, Figure 7 shows the large variability of SSAAE values for every season and atmospheric condition due to the complexity of the different contribution of each type of aerosol measured at CHC. Ealo et al. (2016) have also shown that SSAAE performance in detecting dust is related to the amount of fine particles.

Modifications:

l.521: “In addition to urban and BB influences, the wavelength dependence of the single scattering albedo (SSAAE) measured at CHC highlights a main dust influence during the entire dry season with SSAAE values close to 0.”

Interactive comment on Atmos. Chem. Phys. Discuss., https://doi.org/10.5194/acp-2019-510, 2019.

References:

Arnott, W. P., Hamasha, K., Moosmüller, H., Sheridan, P. J. and Ogren, J. A.: Towards Aerosol Light-Absorption Measurements with a 7-Wavelength Aethalometer: Evaluation with a Photoacoustic Instrument and 3-Wavelength Nephelometer, Aerosol Science and Technology, 39(1), 17–29, doi:10.1080/027868290901972, 2005.

Andreae, M. O. and Gelencsér, A.: Black carbon or brown carbon? The nature of light-absorbing carbonaceous aerosols, Atmospheric Chemistry and Physics, 6(10), 3131–3148, 2006.

Bond, T. C., Habib, G. and Bergstrom, R. W.: Limitations in the enhancement of visible light absorption due to mixing state, Journal of Geophysical Research-Atmospheres, 111, doi:Article, 2006.

Bond, T. C., Doherty, S. J., Fahey, D. W., Forster, P. M., Berntsen, T., DeAngelo, B. J., Flanner, M. G., Ghan, S., Kärcher, B., Koch, D., Kinne, S., Kondo, Y., Quinn, P. K., Sarofim, M. C., Schultz, M. G., Schulz, M., Venkataraman, C., Zhang, H., Zhang, S., Bellouin, N., Guttikunda, S. K., Hopke, P. K., Jacobson, M. Z., Kaiser, J. W., Klimont, Z., Lohmann, U., Schwarz, J. P., Shindell, D., Storelvmo, T., Warren, S. G. and Zender, C. S.: Bounding the role of black carbon in the climate system: A scientific assessment, Journal of Geophysical Research: Atmospheres, 118(11), 5380–5552, doi:10.1002/jgrd.50171, 2013.

Carmona-Moreno, C., Belward, A., Malingreau, J.-P., Hartley, A., Garcia-Alegre, M., Antonovskiy, M., Buchshtaber, V. and Pivovarov, V.: Characterizing interannual variations in global fire calendar using data from Earth observing satellites, Global Change Biology, 11(9), 1537–1555, 2005.

Clarke, A., McNaughton, C., Kapustin, V., Shinozuka, Y., Howell, S., Dibb, J., Zhou, J., Anderson, B., Brekhovskikh, V., Turner, H. and Pinkerton, M.: Biomass burning and pollution aerosol over North America: Organic components and their influence on spectral optical properties and humidification response, J. Geophys. Res. Atmospheres, 112(D12), D12S18, doi:10.1029/2006JD007777, 2007.

Collaud Coen, M., Weingartner, E., Apituley, A., Ceburnis, D., Fierz-Schmidhauser, R., Flentje, H., Henzing, J. S., Jennings, S. G., Moerman, M., Petzold, A., Schmid, O. and Baltensperger, U.: Minimizing light absorption measurement artifacts of the Aethalometer: evaluation of five correction algorithms, Atmospheric Measurement Techniques, 3(2), 457–474, doi:10.5194/amt-3-457-2010, 2010.

Dubovik, O., Holben, B., Eck, T. F., Smirnov, A., Kaufman, Y. J., King, M. D., Tanre, D. and Slutsker, I.: Variability of absorption and optical properties of key aerosol types observed in worldwide locations, J. Atmospheric Sci., 59, 590–608, doi:Review, 2002.

Ealo, M., Alastuey, A., Ripoll, A., Pérez, N., Minguillón, M. C., Querol, X., and Pandolfi, M.: Detection of Saharan dust and biomass burning events using near-real-time intensive aerosol optical properties in the north-western Mediterranean, Atmos. Chem. Phys., 16, 12567–12586, https://doi.org/10.5194/acp-16-12567-2016, 2016.

Ecotech, Aurora 3000 User manual 1.3, November 2009.

Giglio, L., Randerson, J. T. and van der Werf, G. R.: Analysis of daily, monthly, and annual burned area using the fourth-generation global fire emissions database (GFED4), Journal of Geophysical Research: Biogeosciences, 118(1), 317–328, 2013.

Husar, R. B., Husar, J. D. and Martin, L.: Distribution of continental surface aerosol extinction based on visual range data, Atmos. Environ., 34(29–30), 5067–5078, doi:10.1016/S1352-2310(00)00324-1, 2000.

Liousse, C., Cachier, H. and Jennings, S. G.: Optical and thermal measurements of black carbon aerosol content in different environments: Variation of the specific attenuation cross-section, sigma (σ), Atmospheric Environment. Part A. General Topics, 27(8), 1203–1211, 1993.

Rajesh, T. A. and Ramachandran, S.: Black carbon aerosol mass concentration, absorption and single scattering albedo from single and dual spot aethalometers: Radiative implications, Journal of Aerosol Science, 119, 77–90, 2018.

Rose, C., Sellegri, K., Velarde, F., Moreno, I., Ramonet, M., Weinhold, K., Krejci, R., Ginot, P., Andrade, M. and Wiedensohler, A.: Frequent nucleation events at the high altitude station of Chacaltaya (5240 m asl), Bolivia, Atmos. Environ., 102, 18–29, 2015.

Russell, P. B., Bergstrom, R. W., Shinozuka, Y., Clarke, A. D., DeCarlo, P. F., Jimenez, J. L., Livingston, J. M., Redemann, J., Dubovik, O. and Strawa, A.: Absorption Angstrom Exponent in AERONET and related data as an indicator of aerosol composition, Atmospheric Chem. Phys., 10, 1155–1169, doi:10.5194/acp-10-1155-2010, 2010.

Saturno, J., Pöhlker, C., Massabó, D., Brito, J., Carbone, S., Cheng, Y., Chi, X. and Ditas, F.: Comparison of different Aethalometer correction schemes and a reference multi-wavelength absorption technique for ambient aerosol data, Atmos. Meas. Tech., 15, 2017.

Schafer, J. S., Eck, T. F., Holben, B. N., Artaxo, P. and Duarte, A. F.: Characterization of the optical properties of atmospheric aerosols in Amazônia from long-term AERONET monitoring (1993–1995 and 1999–2006), Journal of Geophysical Research: Atmospheres, 113(D4), doi:10.1029/2007JD009319, 2008.

Schmid, O., Artaxo, P., Arnott, W. P., Chand, D., Gatti, L. V., Frank, G. P., Hoffer, A., Schnaiter, M. and Andreae, M. O.: Spectral light absorption by ambient aerosols influenced by biomass burning in the

Amazon Basin. I: Comparison and field calibration of absorption measurement techniques, Atmos. Chem. Phys., 6(11), 3443–3462, doi:10.5194/acp-6-3443-2006, 2006.

Weingartner, E., Saathoff, H., Schnaiter, M., Streit, N., Bitnar, B. and Baltensperger, U.: Absorption of light by soot particles: determination of the absorption coefficient by means of aethalometers, J. Aerosol Sci., 34(10), 1445–1463, doi:10.1016/S0021-8502(03)00359-8, 2003.

Zotter, P., Herich, H., Gysel, M., El-Haddad, I., Zhang, Y., Močnik, G., Hüglin, C., Baltensperger, U., Szidat, S. and Prévôt, A. S.: Evaluation of the absorption Angström exponents for traffic and wood burning in the Aethalometer-based source apportionment using radiocarbon measurements of ambient aerosol, Atmospheric chemistry and physics, 17(6), 4229–4249, 2017.

Anonymous Referee #3

First, authors would like to thank the reviewer for his/her important comments and interesting suggestions. We bieleve they clearly helped highlighting the main conclusions of the paper and extend the interest to regional impacts of aerosol sources in South-America.

As recommend by all reviewers, layers have been renamed in order to justify that the method used only allows to differentiate atmospheric dynamic. Thus, Stable Layer (SC) and Turbulent Layer (TL) are replaced by Stable Condition (SC) and Turbulent Condition (TC).

In the following, authors answer to the reviewer and list modifications made to the paper.

Received and published: 10 September 2019

The paper by Aurelien et al. presents a detailed analysis of aerosol optical properties at a remote site of Andean mountains. The measurements are long-term and, therefore, certainly credible in terms of seasonal cycles, however, the novelty is mainly based on somewhat underexplored and sensitive region and that alone does not constitute scientific novelty. The authors make up for publishable results by careful and thorough data analysis separating dataset to represent stable and turbulent atmospheric layers alongside detailed trajectory analysis. The paper can be accepted for publication after addressing mainly minor comments. Last but not least English can be improved with the help of senior co-authors.

Conclusions could be more concise if a summarising diagram with the main transport patterns and corridors were presented. What matters is not a repeat of study results, but emphasising something about lasting regional impacts. Otherwise, it is just another study of optical properties at a different location.

Answer: Figure has been improved in order to illustrate the main airmasses transported to CHC station according seasons. The main influences for different seasons are discussed from l.274. As the RC3 suggests, this information gives interesting elements to discuss about regional impacts of the different aerosol sources in this particular region. Regional impacts have been highlighted in the final conclusion.

In addition, three tables have been added to summarize ranges of Angström exponent for the different aerosol types (Table 1), to detail the median values of the Angström exponent for each cluster, season and atmospheric stability measured at CHC station (Table 2), and suggest a new Angtsröm exponent definition for the different aerosol types (Table 3).

Modifications:

Figure 4 has been improved.

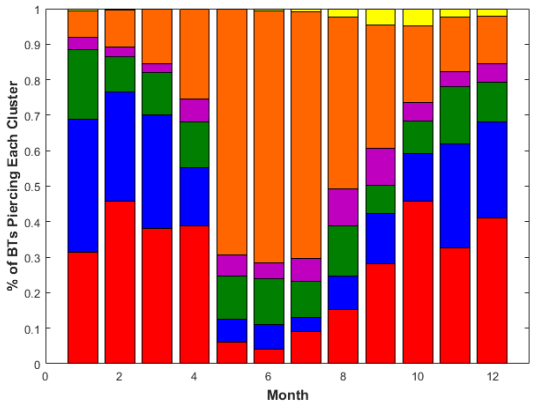

Figure 4: b. Monthly variation of the percentage of back-trajectories (BTs) for each cluster.

Table 1, 2 and 3 have been added.

Aerosol type	SAE	AAE	SSAAE
Dust	Close to 1	Close to 1	Below 0
Urban pollution	Close to 2	Close to 1	Higher than 0
Biomass burning		Close to 2,1	

Table 1: Expected aerosol type and their optical properties for each cluster according season and atmospheric stability.

Cluster	season	SAE	AAE	SSAAE	Aerosol types
NA	WET	2,04 (1,42)	0,58 (0,56)	0,18 (0,15)	urban (dust/urban)
	DRY	1,91 (1,80)	1,00 (1,01)	0,01 (0,004)	urban (dust)
	BB	1,92 (1,87)	1,10 (1,26)	0,03 (0,02)	dust/BB (dust/BB)
SA	WET	1,2 (1,40)	0,74 (0,68)	0,11 (0,11)	urban (urban)
	DRY	1,69 (1,70)	1,04 (0,96)	0,02 (0,03)	dust (dust)
	BB	2,16 (2,02)	1,23 (1,20)	0,005 (0,01)	BB (BB)
LP	WET	1,71 (2,09)	0,86 (0,82)	0,08 (0,10)	urban (urban)
	DRY	1,64 (1,74)	1,05 (1,07)	0,02 (-0,01)	urban (dust/urban)
	BB	1,49 (1,93)	1,09 (1,29)	-0,02 (-0,02)	dust (dust/BB)
ATL	WET	1,93 (2,11)	0,75 (0,65)	0,11 (0,15)	urban (urban)
	DRY	1,77 (1,94)	1,00 (1,05)	-0,001 (0,006)	dust (dust/urban)
	BB	1,80 (1,81)	1,23 (1,08)	0,008 (0,01)	dust/BB (urban)
APO	WET	2,15 (2,04)	0,84 (0,82)	0,11 (0,10)	urban (urban)
	DRY	1,39 (1,38)	1,06 (1,10)	0,006 (-0,02)	dust (dust)
	BB	1,56 (1,61)	1,14 (1,20)	-0,008 (-0,01)	dust/BB (dust/BB)
NES	WET	2,05 (1,67)	0,72 (0,66)	0,13 (0,12)	urban (urban)
	DRY	1,74 (1,83)	1,06 (1,09)	-0,008 (0,003)	dust/urban (dust)
	BB	1,89 (1,80)	0,95 (1,07)	0,002 (0,02)	dust/urban (urban)

Table 2: Median aerosol Angström exponents of turbulent condition (stable condition) for each cluster and seasons measured at the CHC station and resulting aerosol types.

Aerosol type	SAE	AAE	SSAAE
Dust	-	> 0,9	[-0,05 ; 0,05]
Urban pollution	> 1,4	< 0,9	> 0,05
Biomass burning	-	> 1,1	[-0,05 ; 0,05]

Table 3: Updated Angström exponent values expected for aerosol types at the CHC station.

l.127: “As a summary, Table 1 shows expected Angström exponent for dust, urban pollution and Biomass Burning particules according the different referenced works (Dubovik et al., 2002 ; Collaud Coen et al., 2004 ; Clarke et al., 2007 ; Russel et al., 2010). This information has to be taken with caution since source influences are expected homogeneous and have been reported from several regions.”

l.482: “Table 2 summarizes the median Angström exponents measured at the CHC station for turbulent conditions (stable conditions in parenthesis). According to these values and as discussed above, aerosol types for the turbulent conditions (and stable conditions in parenthesis) are given.”

l.525: “A new Angtsröm exponent classification can then be defined for measurement at the CHC station and is reported Table 3. Thresholds are close to the ones proposed by previous works (Dubovik et al., 2002 ; Collaud Coen et al., 2004 ; Clarke et al., 2007 ; Russel et al., 2010) but adapted to CHC’s instruments and particular atmospheric conditions.”

l.4503: “The present study clearly demonstrates the regional impacts of these activities.”

l.505: “The present study has hence demonstrated that BB particles are efficiently transported to the higher part of the troposphere (Stable conditions) and over long distances (more than 300 km long).”

l.510: “One of the main aerosol sources in the Bolivian plateau is the urban area of La Paz / El Alto.”

l.520: “Finally, the arid plateau of the region has also demonstrated regional impact. In addition to urban and BB influences, the wavelength dependence of the single scattering albedo (SSAAE) measured at CHC highlights a main dust influence during the entire dry season with SSAAE values close to 0.”

Minor comments

Line 31. Resulting in lower atmospheric...

Answer: In the final version, this sentence has been deleted.

Line 33. different aerosol sources.

Answer: In the final version, this sentence has been deleted.

Line 35. on average, instead of "in average".

Answer: Correction made.

Modification:

l.39: “[...] extinction coefficients are on average [...]”

Line 41. ...increase in the extinction...

Answer: Correction made.

Modification:

l.54: “28% to 80% increase in the extinction”

Line 44. How far away?

Answer: Scales still difficult to describe when only one in-situ station is used in addition to back-trajectories. In the present study, “long distance influences” is used for aerosol particles transported several hundreds of kilometres far from their sources whereas “local influence” is linked to aerosol particles transported less than 100 km from their sources. Additional ground based measurements could help to locate with more detail aerosol sources and satellite measurements could give more information on their long distance transport.

Modification:

l.46: “[...] far away from their sources [...]” is replaced by “[...] to a remote site [...]”

Is stable layer normally the upper layer above the boundary layer or is it free troposphere? I understand it is based on statistical treatment, but the abstract should convey the message without reading all the details.

Answer: From the method based on the local dynamic of the atmosphere and the impossibility to access to the vertical distribution of aerosol for the full period, stable and turbulent conditions are used in this study to differentiate atmospheric layers. Hence, it is not possible to attribute stable and turbulent conditions to unique common tropospheric layers. A sentence is added on the abstract to make this step clearer.

Modification:

l.58: “Results are also separated from distinct atmospheric conditions as stable and turbulent, with associated properties of the free troposphere and the planetary boundary layer”

Line 106-113. There have to be goals, not summary and justification of what and how the study has done.

Answer: The paragraph has been modified according to these suggestions.

Modification:

l.133: “Monthly and diurnal variations of extensive optical properties (related to particle concentration) and intensive optical properties (related to particle chemistry) are firstly shown. A robust method based on the measurement of the atmospheric stability is then applied to distinguish atmospheric conditions (stable and turbulent). Finally, back-trajectory analysis and optical wavelength dependences are presented to identify impacts of local and regional aerosol sources.”

Figure 1. In insert would help to visualise in the larger region, especially tha the Figure covers only appr. 50x50km.

Answer: A larger view of the topography is added to figure 1.

Modification:

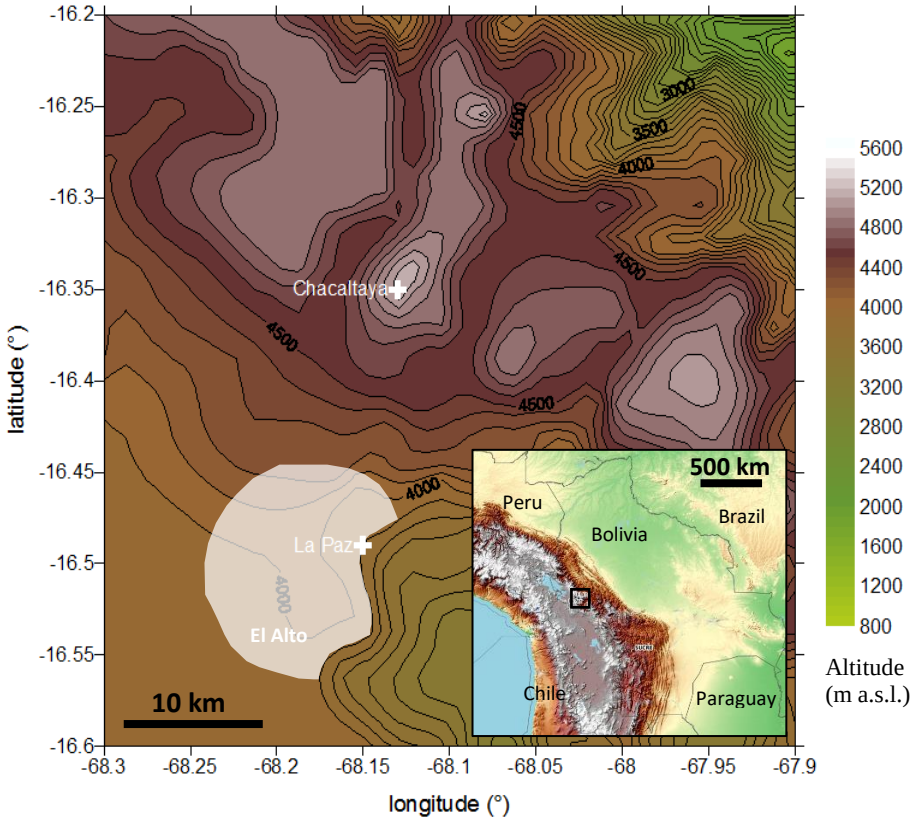

Figure 1: Topographic description of La Paz and Chacaltaya region, and Bolivia in the lower right panel. The black rectangle on the small panel represents La Paz region. The urban area of La Paz-El Alto (marked as white shading) lies in the Altiplano high-plateau at around 4000 m a.s.l..

Line 125. The papers deals with impacts over much larger region, therefore, it is important to describe that larger region, e.g. extending to 200km.

Answer: As discussed in previous remarks, long range transport is related to several hundreds of kilometres. Precisions have been added to the text.

Line 193. Use past tense as measurements represent the past not present day.

Answer: Correction made.

Modification:

l.250: “This 3-day example showed that [...]”

Line 276. Correlation is a scientific term, therefore, cannot "correlate to seasons". Use "...values exhibited typical seasonal variation".

Answer: Correction made.

Modification:

l.347: “[...] variations of AAE and SSAAE values exhibited typical seasonal variation.”

Line 327. I am not sure I follow why SL particles are aged longer and transported farther. Please elaborate.

Answer: Aerosol particles reaching high altitudes are subject to a more stable atmosphere with strong horizontal circulation and weak vertical motions. Hence, especially small particles (diameters around 1 µm) can be aged longer and transported farther.

Modification:

l.399: "[...] SC aerosol particles are aged longer and transported farther than TC particles due to less scavenging effects."

Interactive comment on Atmos. Chem. Phys. Discuss., https://doi.org/10.5194/acp-2019-510,2019

References:

Clarke, A., McNaughton, C., Kapustin, V., Shinozuka, Y., Howell, S., Dibb, J., Zhou, J., Anderson, B., Brekhovskikh, V., Turner, H. and Pinkerton, M.: Biomass burning and pollution aerosol over North America: Organic components and their influence on spectral optical properties and humidification response, J. Geophys. Res. Atmospheres, 112(D12), D12S18, doi:10.1029/2006JD007777, 2007.

Collaud Coen, M., Weingartner, E., Apituley, A., Ceburnis, D., Fierz-Schmidhauser, R., Flentje, H., Henzing, J. S., Jennings, S. G., Moerman, M., Petzold, A., Schmid, O. and Baltensperger, U.: Minimizing light absorption measurement artifacts of the Aethalometer: evaluation of five correction algorithms, Atmospheric Measurement Techniques, 3(2), 457–474, doi:10.5194/amt-3-457-2010, 2010.

Dubovik, O., Holben, B., Eck, T. F., Smirnov, A., Kaufman, Y. J., King, M. D., Tanre, D. and Slutsker, I.: Variability of absorption and optical properties of key aerosol types observed in worldwide locations, J. Atmospheric Sci., 59, 590–608, doi:Review, 2002.Russell, P. B., Bergstrom, R. W., Shinozuka, Y., Clarke, A. D., DeCarlo, P. F., Jimenez, J. L., Livingston, J. M., Redemann, J., Dubovik, O. and Strawa, A.: Absorption Angstrom Exponent in AERONET and related data as an indicator of aerosol composition, Atmospheric Chem. Phys., 10, 1155–1169, doi:10.5194/acp-10-1155-2010, 2010.

Russell, P. B., Bergstrom, R. W., Shinozuka, Y., Clarke, A. D., DeCarlo, P. F., Jimenez, J. L., Livingston, J. M., Redemann, J., Dubovik, O. and Strawa, A.: Absorption Angstrom Exponent in AERONET and related data as an indicator of aerosol composition, Atmospheric Chem. Phys., 10, 1155–1169, doi:10.5194/acp-10-1155-2010, 2010.